NTNU

Norwegian University of
Science and Technology

Positive Lightning Impulses in a Rod-Plane Gap with insulating Barriers

Measurements of electric withstand voltage in air for configurations with insulating barriers

Kristian Lie Hokstad

Master of Energy and Environmental Engineering
Submission date: July 2016
Supervisor: Frank Mauseth, ELKRAFT

Norwegian University of Science and Technology
Department of Electric Power Engineering

Problem description

In today's medium and high voltage equipment, SF_6 is the main insulation and quenching medium. However, there is a growing concern around its potency as a greenhouse gas. Therefore, using atmospheric air as the insulating medium has lately been a priority for producers of medium and high voltage equipment. The withstand voltage of air is lower than SF_6, and a challenge for equipment designers is to make air insulated equipment with a compact and competitive design. Barriers are frequently used in the design to increase the path of the streamer and thus increasing the withstand voltage.

During the design process FEM software analysis is used to calculate the electrostatic field strength on the different components in the equipment. However, knowing the electrostatic field distribution is not sufficient to predict the withstand voltage. It is also necessary to model the discharge processes including inception and propagation of streamers.

The main topic of the project work will be the study of inception and propagation of streamers leading to breakdown in air insulated rod-plane gaps with insulating barriers. The work will consist of both laboratory measurements and electromagnetic simulations of breakdown in a rod-plane gap with insulating barriers. The results will be used to verify formulas for predicting withstand voltages.

This project is part of a four year research project on "Electrical insulation with low-GWP gases" funded by the Norwegian Research Fund and ABB AS, Skien, Norway and ABB Ltd. Switzerland.

Preface

The goal of this project thesis is to document, predict and explain the observed increasing withstand voltage when a rod-plane gap is insulated with polycarbonate barriers. The thesis will introduce some theory on the breakdown of gases by streamer and Townsend mechanisms. The barrier effects and results are presented in figures and tables, and the results are discussed.

I would like to thank the project supervisors, Frank Mauseth, Associate Professor at the Department of Electric Power Engineering of the Norwegian University of Technology and Science, and Atle Pedersen, Research Manager at SINTEF Energy Research for their help and support.

I would also like to thank fellow students Vegard Skonseng Bjerketvedt, Eirik Grytli and Kristine Korneliussen for beeing my security backup and keeping me company in the high voltage lab.

Abstract

Today's design and manufacturing of high voltage equipment focuses increasingly on a shift away from SF_6 as a quenching and isolation medium. SF_6 is has a detrimental effect on the atmosphere's greenhouse potential. Bans or regulations regarding SF_6 may well be imposed on the industry in the future. In order to replace SF_6 with air as insulation, more research is needed to achieve compact and efficient designs.

The goal of this master thesis has been to investigate the effect of barriers on the withstand voltage in rod-plane gaps, with atmospheric air, subjected to positive high voltage impulses. The high voltage electrode was a rod with a spherical tip and a diameter of 7 mm. The barriers used as insulation were made out of Lexan polycarbonate plates and measured 1 mm $\times$ 600 mm $\times$ 600 mm. The 50% breakdown voltage, the standard deviation and the withstand voltage have been determined using the up- and down-method. The barriers were tested in several configurations, changing both the horizontal and vertical placement of the barrier in the rod-plane gap. In addition to physical experiments, these configurations have been investigated in terms of electric background field calculations in COMSOL, as well as streamer inception voltage calculations in MATLAB.

The results show an increase in the withstand voltage of up to 28% for the configuration with the largest barrier protrusion. The optimal barrier position has been found to be close to the high voltage rod. However, a relative decrease in the withstand voltage is observed when the rod is touching the barrier. This can be explained by a strong tangential field allowing the streamer to propagate along the surface of the barrier. For a small barrier, protruding 0 mm from the tip of the rod, the withstand voltage is lower than that of a barrier-less rod plane gap when the barrier touches the rod. A sharp increase of above 10% in the withstand voltage is shown in a barrier with a 0 mm overlap, by simply moving the barrier 10 mm closer to the high voltage rod. This can to some degree be explained by applying electric potential to the barriers in the background field distributions.

It has been shown that the withstand voltage can be predicted to some extent with a very simple formula for the configurations with the largest barrier protrusions. A method of predicting withstand voltage based on streamer inception calculation in several steps, with electric field distribution calculations has been suggested.

Sammendrag

I dagens marked for høyspenningsanlegg er det et økende fokus på å kvitte seg med SF_6 som isolasjons-medium. SF_6 er en meget potent drivhus-gass som påvirker atmosfærens oppvarmings-potensiale svært kraftig. Industrien kan oppleve å bli møtt med strenge restriksjoner og krav rundt bruk av SF_6 i fremtiden. For å erstatte SF_6 med luft som isolasjonsmateriale trengs mer forskning på å oppnå kompakte og effektive design.

Målet med denne masteroppgaven er å undersøke virkiningen av barrierer i et stang-plate-gap, med atmosfærisk luft, utsatt for positive spenningsimpulser. 50%-verdien for gjennombruddspenning, standard-avvik og elektrisk holdfasthet har blitt bestemt ved hjelp av opp- og ned-metoden. Høyspenningslektroden er en metallstang med sfærisk tupp og en diameter på 7 mm. De isolerende barrierene består av Lexan polykarbonat-plater og har dimensjonene 1 mm $\times$ 600 mm $\times$ 600 mm. Barrierene ble testet i flere konfgiurasjoner ved å endre posisjon både horisontalt og vertikalt i stang-plate-gapet. I tillegg til de fysiske eksperimentene har de samme konfigurasjonene blitt undersøkt med tanke på beregninger av det elektriske bakgrunnsfeltet i COMSOL og beregninger av streamer tenn-spenning i MATLAB.

Resultatene viser en økning i elektrisk holdfasthet på opp til 28% for konfigurasjonen med det største fremspringet på barrieren. Optimal barriere-posisjon har blitt vist å være nære høyspennings-elektroden. Det er derimot vist en betydelig relativ svekkelse av den elektriske holdfastheten når barrieren rører høyspenningselektroden. Dette kan forklares ut fra det sterke tangetielle feltet som lar streameren propagere langs med barriere-flaten. For en liten barriere, med 0 mm fremspring, er det vist en betraktelig lavere holdfasthet sammenlignet med det barriere-løse gapet når barrieren rører elektroden. For barrierer med 0 mm fremspring er det vist en betraktelig økning av holdfasteten, som er oppnådd bare ved å heve barrieren 10 mm. Dette kan delvis forklares ved å se på hvordan ladning på barrieren svekker feltet mellom stang og barriere og endrer fordelingen av det elektriske bakgrunnsfeltet.

Det er vist hvordan den elektriske holdfastheten kan beregnes med en svært enkel formel for de største barriere-fremspringene. En metode for å predikere holdfasthet basert på beregninger streamer tenn-spenninger i flere trinn er foreslått.

Contents

Problem description i
Preface iii
Abstract v
Sammendrag vii

1 Introduction **1**

2 Theory **3**
2.1 Air as insulation 3
2.2 Townsend's breakdown mechanism in air 3
2.2.1 Townsend's first coefficient 4
2.2.2 Townsend's second coefficient 4
2.3 Streamer propagation 4
2.3.1 The streamer path 6
2.4 The effect of barriers 8
2.5 Electric breakdown as a stochastic variable 9
2.5.1 Linear regression 10
2.5.2 Breakdown and withstand voltage 10

3 Method **13**
3.1 Experimental set-up 13
3.1.1 Impulse voltage generator 13
3.1.2 Measuring equipment 15
3.1.3 Measuring circuit 16
3.1.4 Photography 17
3.1.5 Gap arrangement 17
3.2 Experimental method 19
3.2.1 The up-and-down method 19
3.2.2 Barrier charge measurements 20
3.2.3 Correcting for air density 21
3.3 Field distribution calculations 21
3.3.1 COMSOL model properties 21
3.3.2 Parameter sweeps 22
3.4 Streamer inception voltage calculation 23

4 Results and Discussion **25**
4.1 Experimental lab results . . . 25
4.1.1 Breakdown voltage measurements . . . 25
4.1.2 Field strength measurements . . . 27
4.1.3 Streamer paths at breakdown. . . . 29
4.2 Field distribution calculations . . . 30
4.3 Inception voltage calculations . . . 32
4.4 Sources of error . . . 34
4.4.1 Barrier placements and gap distances . . . 34
4.4.2 Oscilloscope readings . . . 35
4.4.3 Component values . . . 36
4.4.4 Surface charge . . . 36
4.4.5 Standard deviations and breakdown regions . . . 36

5 Conclusion **37**

6 Further Work **39**

Bibliography **41**

A Equipment and serial numbers **1**

B MATLAB source code **3**
B.1 Integration of α_{eff} . . . 3
B.2 Field scaling function . . . 4
B.3 Streamer matrix sorting . . . 4
B.4 Inception voltage calculation . . . 5

C Inception voltage calculations **7**

D Barrier voltage approximations **9**

E Pictures of streamer paths at breakdown **11**

F Up- and down-method breakdown regions **13**

List of Figures

2.1 Positive withstand voltage U_W in relation to field homogeneity and gap distance in a sphere-plate arrangement [1]. P denotes the transition from a weakly to a strongly inhomogenous field. Q denotes the point where the graph is valid for very long distances (1-2 m) or in the precence of a dielectric surface. 6

2.2 Experimental set up parameters. p is the barrier protrusion from the centre of the rod to the edge of the barrier. d is the barrier height from the ground electrode to the top of the barrier. t is the thickness of the barrier. The distance from the barrier to the high voltage electrode is denoted d'. 7

2.3 Possible streamer paths. Path (a) shows the streamer growing straight down to the barrier and following the edges of the barrier. Path (b) shows the geometrically shortest distance, x_s. Path (c) show a streamer following an imagined field line which is affected by a charged barrier. 8

3.1 Circuit drawing of the impulse generator used to apply impulses to the test object. The most important components are the high voltage transformer, the charging capacitors, and the sphere gaps. The symbols in the drawing are explained in table 3.1. [2] 14

3.2 Captured images from the oscilloscope showing a test with and without electrical breakdown respectively. The signal amplitudes and rise times are measured with the cursor measuring device. The polarity of the impulses are arbitrary, the figure is only meant to illustrate the measurement of amplitude and rise times. 15

3.3 Measuring circuit placed between the impulse generator and oscilloscope. The circuit is a series of voltage dividers in order to avoid large voltages from the impulse generator directly on the scope. The wave impedance Z_k is the characteristic impedance of the cable to the oscilloscope. 17

3.4 Test arrangement. A) Shows the rod length and diameter. B) Shows the length, width and thickness of the barriers. NB: The thickness of the barriers used in most of the tests in this thesis is 1 mm. C) Shows the barrier support system and dimensions. D) Shows the mounted test arrangement. [3] 18
3.5 A conceptual example of a test done with the up-and down method. The impulse voltage is adjusted up or down by ΔU depends on whether the impulse results in a breakdown or not. The blue line marks the average of the breakdown voltages in the valid area (the ramping up is not included). 20
3.6 Geometry of the COMSOL model. The high voltage rod is highlighted and cut in two by the mirroring surface. Below the rod is the insulating barrier, protruding 0 mm from the centre of the rod. The blue shaded area shows the regions of the model where the electric field exceeds 0.54 $\frac{kV}{mm}$ for an arbitrary rod voltage. The coloured lines are the electric field lines and the colour grading signifies the magnitude of the electric field. 22

4.1 Withstand voltages for all the configurations with 1 mm barrier thickness. The reference is the withstand voltage in the gap without a barrier. The results can also be seen in table 4.1. 27
4.2 0 mm barrier protrusion with measured breakdown and withstand voltages. The standard deviation is shown in the vertical error bars. The reference is the breakdown voltage in the gap without a barrier. The results can also be seen in table 4.1. The barrier thickness is 1 mm. 28
4.3 40 mm barrier protrusion with measured breakdown and withstand voltages. The standard deviation is shown in the vertical error bars. The reference is the breakdown voltage in the gap without a barrier. The results can also be seen in table 4.1. The thickness of the barrier is 1 mm. 29
4.4 Withstand and breakdown voltages for constant barrier heights of 30 and 50 mm with varying protrusions The barrier thickness is 1 mm. The standard deviation is shown in the vertical error bars. The reference is the breakdown voltage in the gap without a barrier. The results can also be seen in table 4.1. 30
4.5 Measured field strength on the barrier after an impulse. The graph shows the charge magnitude over time on the barrier, with and without a breakdown respectively. The measuring probe was placed 100 mm above the barrier and directly above the tip of the rod. 31
4.6 Field distributions with applied breakdown voltage U_{BD} on the rod. The white area signifies the region where the electric field E_{norm} ≥ 0.54 $\frac{kV}{mm}$. The color code ranges 0.54 (dark blue) to 6 from $\frac{kV}{mm}$ (dark red). Figures (a) to (d) show applied rod voltage $U_{BD} = 85$ kV, barrier height $d = 30$ mm, barrier protrusion $p = 0$ mm, barrier thickness, $t = 1$ mm. 32

4.7 Field distributions with applied breakdown voltage U_{BD} on the rod. The white area signifies the region where the electric field $E_{norm} \geq 0.54\ \frac{kV}{mm}$. The color code ranges 0.54 (dark blue) to 6 from $\frac{kV}{mm}$ (dark red). Figures (a) to (d) show applied rod voltage $U_{BD} = 75$ kV, barrier height $d = 20$ mm, barrier protrusion $p = 0$ mm, barrier thickness, $t = 1$ mm. 33
4.8 Calculated inception voltages for the configurations with 0, 20 and 40 mm barrier protrusions. The barrier thickness is kept at 1 mm. The results can also be seen in table 4.5. 35

C.1 Plotted electric field strength against the length of the field line. The field distribution is from a configuration with 0 mm barrier protrusion and 30 mm barrier height. The thickness of the barrier is 1 mm. The length of the streamer that contributes to the integral is for this instance 2.8 mm. 7
C.2 Inception voltage calculation with basis in a barrier with no charge (blue) and a barrier with a 300 V initial charge (red) in the COMSOL background field calculations. The barrier heights are adjusted from 20 mm to 60 mm in increments of 10 mm. The protrusion is 0 mm and the thickness is 1 mm. 8

D.1 The result of a parametric sweep to examine which applied voltage corresponds to the measured field strength after an impulse. The data range shown in blue shows the area where the field strength is $0.115\ \frac{kV}{mm}$, which is the maximum field strength measured after an impulse that did not result in breakdown. 9
D.2 The result of a parametric sweep to examine which applied voltage corresponds to the measured field strength after an impulse. The data range shown in blue shows the area where the field strength is $0.043\ \frac{kV}{mm}$, which is the maximum field strength measured after an impulse that did result in breakdown. 10

E.1 Photographed streamer paths at flash over for positive voltages. The barrier distance d is fixed to 20 mm. The barrier is protruding 10 mm from the centre of the rod. The thickness of the barrier is 5 mm. 12

F.1 Example of a test where the region of the breakdown voltage is hard to ascertain. The breakdown voltage seems to drop in the first 7 impulses, then rise by a magnitude of 10 kV.The values were obtained during a single day with negligible changes in humidity and air pressure. The values from this test were rejected. 13

List of Tables

3.1 The component names and values of impulse generator as seen in figure 3.1 [2]. 14

4.1 Measured withstand voltage, U_{WS}, breakdown voltage, U_{BD}, and standard deviation, σ, for impulses with barriers protruding 0, 20 and 40 mm from the centre of the rod. 26

4.2 Improvement to withstand voltage in comparison to the withstand voltage in a barrier-less gap. The barrier thickness for all instances is 1 mm. 26

4.3 The shortest streamer path x_s calculated from Equation 2.6, predicted withstand voltage, U_{pred}, calculated from Equation 2.7 and the fault of the prediction compared to the measured results in per cent. Negative faults predicated too high a withstand voltage. 28

4.4 Calculated barrier charge required to obtain a contiguous electrical field with field strength $E_{norm} \geq 0.54\ \frac{kV}{mm}$. The voltage applied to the rod in the configurations are the breakdown voltages observed experimentally (table 4.1). The calculations are done for varying values of barrier protrusion, p, and barrier height from the ground, d, with constant barrier thickness 1 mm. The sweeps are done in increments of 1 kV. 34

4.5 Calculated rod voltages needed to instigate streamer inception according to [1]. The calculations are done for varying values of barrier protrusion, p, and barrier height from the ground, d. The barrier thickness is kept constant at 1 mm. Background field calcultations are conducted in COMSOL and post processed in MATLAB. The results can also be seen in figure 4.8. 35

A.1 Equipment names and serial numbers 1

Chapter 1

Introduction

High voltage equipment which is constrained by space concerns need to be compact in order to be competitive. In today's market, SF_6 is the dominating insulation medium for such compact equipment. With a society that places an increasing value on environmental concerns, SF_6 may prove to become an unwanted and expensive alternative. SF_6 may be affected in the future by for instance the EU F-gas regulations, regarding fluorinated greenhouse gases. This is due to the fact that SF_6 is an extremely potent greenhouse gas. When considering other insulation media, air is a natural choice. Notable advantages of air as an insulation medium are the availability and non-toxicity. However, both the withstand voltage and quenching capabilities of air are significantly poorer than those of SF_6.

To increase the withstand voltage of air insulated systems it may be a viable option to employ insulating barriers in the air gap. These barriers can increase the withstand voltage by increasing the path the streamer has to travel. The barrier also attracts charge which can alter the field distribution, further increasing the withstand voltage. Literature on the subject of barriers suggest that the withstand voltage for positive voltages can be increased up to a factor of 3 when comparing with a barrier-less gap. [4]. The goal of this project thesis is to investigate the effect of thinner of 1 mm barriers when subjected to positive high voltage impulses.

The effect of the barrier on the withstand voltage has been investigated by a series of impulse voltage tests on a rod plane gap. This has been done for barrier configurations, altering the barrier position both horizontally and vertically. The tests have been conducted according to the up-and-down method, a popular statistical method for such experimental work. The up and down method requires few repetitions to give a relatively accurate statistical result. An attempt has been made to estimate the withstand voltage for different barrier topologies based on the barrier-less withstand voltages and an estimated streamer path. A model of the experiment has been built in COMSOL and field calculations are used to try to explain the observed phenomena. The streamer inception voltages for all barrier configurations has been calculated based on the background field calculations.

Chapter 2

Theory

2.1 Air as insulation

Atmospheric air is the cheapest and most available insulation medium known. Its main advantages is that it poses no threat to the environment, and it is free and self healing. Air as an electric insulation medium becomes more interesting as there is a growing concern around the use of Sulphur hexafluoride (SF_6) and its contribution to the green house effect. Climate scientists have estimated that SF_6 has a global warming potential of 22 800 over a 100 year period compared to that of CO_2 [5]. SF_6 is listed in the Kyoto Protocol as a greenhouse gas that should have limited or lowered emissions [6].

2.2 Townsend's breakdown mechanism in air

John Sealy Townsend developed his theory on electrical breakdown in gases between 1897 and 1901. Townsend's mechanism explains how electrons affected by an electric field can form so called electric avalanches that lead to electrical breakdown. The current i_e flowing between two electrodes insulated by air can be approximated as:

$$i \approx i_e = \frac{i_0 e^{\alpha d}}{1 - \gamma(e^{\alpha d} - 1)} \tag{2.1}$$

i_0 is the photoelectric current generated at the surface of the cathode. An infinite current, thus an electric breakdown, will occur when the denominator is zero. From this Townsend's breakdown criterion for air is formulated [7]:

$$\gamma(e^{\alpha d} - 1) = 1 \tag{2.2}$$

Here α and γ are Townsend's first and second coefficients respectively. The distance d is the distance between the anode and the cathode. For electronegative gasses, such as SF_6, the breakdown criterion is also affected by the likelihood that the

electrons are absorbed by the gas. This probability coefficient is usually named η. N_2 however, which is the main component of air, is considered an electro-positive gas, so η will not be discussed further here.

2.2.1 Townsend's first coefficient

When an external electric field is applied the electrons in the gas will experience coulomb forces given by $F = qE$. This force will result in a net movement against the direction of the electric field towards the anode. This movement is called *drift* and the velocity with which the electrons move is called *drift velocity*[7]. The drifting electrons will have a statistical chance of colliding with other molecules. When such a collision occurs, the electron will yield some of its energy (collisions in ideal gasses are close to perfect elastic collisions) to the molecule it collides with. This energy transfer may cause the molecule to release a new electron which can start the same process over again.

The energy transferred to an electron during a collision is proportional to the field strength E and the mean free path λ_e. The mean free path is inversely proportional to the gas pressure p at a given temperature. Thus, the probability that a collision is ionizing is a function of $\frac{E}{p}$. This probability is known as Townsend's first ionization coefficient; α and is given per unit length.

2.2.2 Townsend's second coefficient

As the cathode is hit repeatedly by positive ions and photons, there is a chance that a secondary electron will be released from the cathode. Townsend's second ionization coefficient, γ, gives the probability that one electron is released from the cathode for each positive ion generated. If the cathode ionization is to contribute to the avalanche, it has to release two electrons; one to negate the charge of the positive ion and one to launch as a secondary electron. Townsend's second coefficient is also a function of the electrical field strength, the dielectric material and the gas pressure [7].

2.3 Streamer propagation

The theory of streamer discharges was conceived after it became clear that Townsend's theory was inconsistent with experimental results. For experiments with higher electrical field stress, pressure and longer gap distances, another theory had to be developed. This theory on breakdown from a single electron avalanche was proposed independently by Raether [8] and Loeb [9] in 1939. Meek also presented his theory on spark discharge [10] in 1940. This new theory sufficiently explained the experimental results.

An electric avalanche becomes self propagating when the number of electrons in

it reaches a critical size, N_c. Accelerated electrons will ionize gas atoms, releasing new electric avalanches and intensify the space charge further. The feedback process occurs when released photons collide with gas atoms close by, causing further ionization in a step wise manner. This process is, compared to Townsend's mechanism, a very fast one. The typical breakdown from a streamer process occurs within 1 - 100 ns of the initial critical electron formation [11]. Townsend's breakdown mechanism, on the other hand, has a breakdown time in the order of μs from the initial electron avalanche. This difference in the time to breakdown also explains why the γ-feedback mechanism at the cathode can not be required for a breakdown with the streamer mechanism. The time span is too short for the ions to move back to the cathode and release secondary electrons in the streamer mechanism. The final breakdown plasma channel is sharp and narrow, compared to the diffuse "cloud" which can be observed from the breakdowns caused by Townsend's mechanism.

The streamer inception criterion is given by Equation 2.3

$$\int_{\Gamma} \alpha_{\text{eff}} dx = ln(N_c) \tag{2.3}$$

Here, $\alpha_{\text{eff}}(E)$ is the effective ionization coefficient dependent on the electrical field strength. $\alpha_{\text{eff}}(E)$ includes ionization, electron attachment and electron detachment. This integral is performed along the path Γ where $\alpha_{\text{eff}}(E) > 0$, starting at the point with the maximum field strength and ending where $\alpha_{\text{eff}}(E_c) = 0$ [1]. E_c is the electric field strength where the ionization and recombination probabilites are equal. For atmospheric air E_c is typically around 2.5 $\frac{kV}{mm}$ [12]. The value of the streamer constant $ln(N_c)$, sometimes called K, is subject to some controversy. Various literature assigns $ln(N_c)$ values from 18.14 ([1]) to 10 ([12]).

The minimum voltage required for the occurrence of a breakdown in a sphere-plane arrangement, U_W, can be estimated from equation 2.4 [1]. This equation is assumed to be valid for gap distances of 40-50 mm.

$$U_W = U_0 + d \cdot E_{st} \tag{2.4}$$

The breakdown voltage, U_W, is determined by the voltage required for the streamer head to initiate breakdown U_0, the distance d of the rod-plane gap, and the internal field strength of the streamer, E_{st}. The voltage U_0 is estimated to be in the magnitude of $U_0 \approx 20-30\ kV$, which is the streamer head potential that is required to generate a breakdown [1]. For a positive impulse, the strength of the streamer propagation field is $E_{st} = 0.54\ \frac{kV}{mm}$. A negative impulse requires a higher field strength of $E_{st} = 1.2\ \frac{kV}{mm}$ [1]. This approximation is valid in regions with a high degree of inhomogeneity i.e. for rod-gap distances of 40 mm and higher. Figure 2.1 shows the withstand voltage of air in a sphere-plane arrangement with the red line representing U_W. The withstand voltage is determined for three different stages of streamer development. The point P marks the limit between a weakly and a strongly inhomogeneous field. For a shorter distance, d, the streamer inception

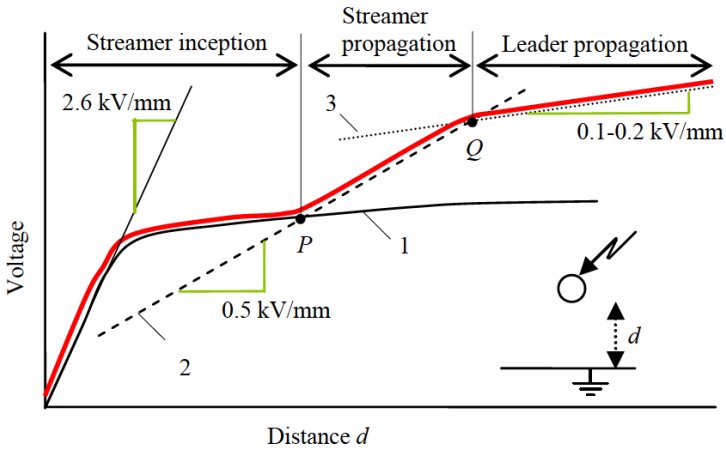

Figure 2.1: Positive withstand voltage U_W in relation to field homogeneity and gap distance in a sphere-plate arrangement [1]. P denotes the transition from a weakly to a strongly inhomogenous field. Q denotes the point where the graph is valid for very long distances (1-2 m) or in the precence of a dielectric surface.

leads to an immediate discharge. The point Q marks the transition to the leader region. This region is valid for long gaps of 1-2 m or in the presence of a dielectric surface. In this case d is the discharge path along the dielectric surface and not the gap between. The voltage drop in a leader is lower than in a streamer and may thus propagate over a larger distance [1].

2.3.1 The streamer path

The path of the streamer propagation is an important parameter when trying to estimate the breakdown voltage. The withstand voltage increases with gap distance which can be seen in figure 2.1. According to most literature the streamer starts at the point of the highest electrical field strength along an electric field line $-\vec{\nabla}V$ of the background field. A proposed streamer propagation model can be seen in equation 2.5 [1].

$$\vec{v} = A \cdot \vec{E} + B \cdot \vec{\nabla} \cdot \vec{E}^2 \tag{2.5}$$

This model suggests that the streamer follows the field line until the field strength is too low. The streamer will then either stop or deflect and follow the boundary of this region in the direction of a higher field strength. In Equation 2.5, this is done by setting the scalar $A(E < 0.54\frac{kV}{mm}) = 0$. The terms A in combination with B must be determined from experiments or basic theory in order to achieve streamer propagation within an observed region [1]. The streamer stops when either $\vec{\nabla} \cdot \vec{E}^2 \propto \vec{E}$ or it reaches the electrode causing a breakdown.

In experiments it has been observed that the streamer does not always follow this model. One suggestion is that the streamer propagates along the maximum field and crosses the field lines. If this is the case, the path of the streamer can be found by connecting the points of the highest field strengths for each equipotential curve [1].

By inserting an insulating barrier in the streamer path, the streamer is forced to either find a new route around the barrier, or penetrate it. Either way, the withstand voltage is increased for smaller air gaps. This is an advantage when compact designs are required. Figure 2.3 shows three possible streamer paths. The shortest path is shown as "Path (b)" where the streamer propagates directly towards the edge of the barrier and down to the ground electrode. Another possible route is for the streamer to travel vertically down to the barrier and then move "around" it down to ground. A third possibility is for the streamer to more or less follow the electric field line seen in figure 2.3 as "Path (c)". If the streamer propagates along the shortest path, the distance it travels can be calculated from equation 2.6. The symbols in Equation 2.6 are explained in figure 2.2. Since the barrier thickness is kept constant, the thickness parameter, t, is not included in Equation 2.6, the thickness is however included in the distance $d - d'$. Distances can be seen in figure 2.2.

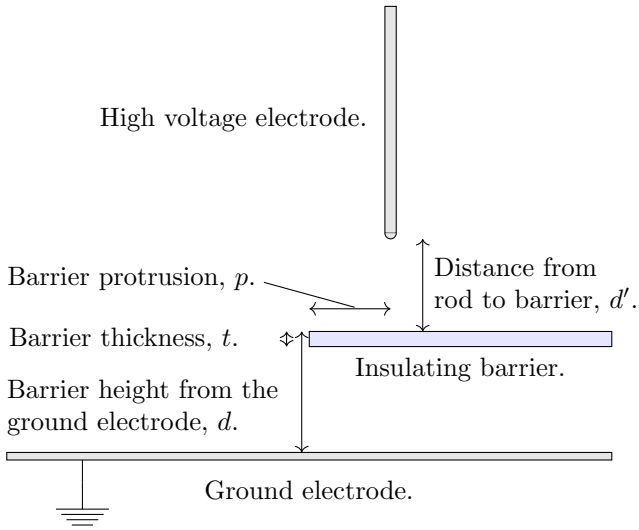

Figure 2.2: Experimental set up parameters. p is the barrier protrusion from the centre of the rod to the edge of the barrier. d is the barrier height from the ground electrode to the top of the barrier. t is the thickness of the barrier. The distance from the barrier to the high voltage electrode is denoted d'.

$$x_s = d + \sqrt{d'^2 + p^2} \tag{2.6}$$

With this new distance a theoretical new withstand voltage based on the increased streamer path can be estimated with a modification of Equation 2.4. The new predicted voltage estimation can be seen in Equation 2.7 [3].

$$U_{\text{pred}} = U_{\text{no barrier}} + (x_s - (d + d')) \cdot E_{st} \tag{2.7}$$

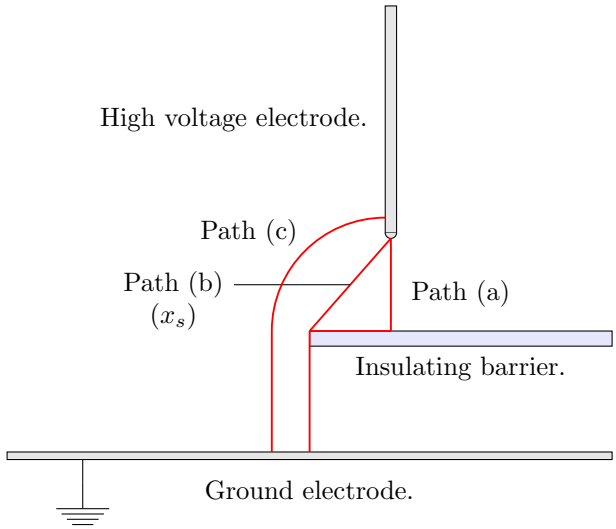

Figure 2.3: Possible streamer paths. Path (a) shows the streamer growing straight down to the barrier and following the edges of the barrier. Path (b) shows the geometrically shortest distance, x_s. Path (c) show a streamer following an imagined field line which is affected by a charged barrier.

2.4 The effect of barriers

The introduction of a barrier in the gap has shown to increase the withstand voltage [4]. This increase is not due to a change in the background field. The background field distribution will be relatively unaffected by the barrier, prior to an eventual charge of the barrier.

The increase in the withstand voltage is associated to a redistribution of the field in the gap. This redistribution is caused by a space-charge field which originates from ionization from impacts close to the tip of the rod and accumulates on the barrier surface [4]. For positive applied voltages the ionization takes place in the

region around the tip of the rod. The ionization results in the formation of positive charge carriers, which is the ionized gas molecules and negative carriers, which are electrons. The heavier and slower positive charge carriers will linger longer around the tip reducing the field strength, increasing the withstand voltage. The positive ions will drift towards the barrier and eventually distribute evenly [4]. This positive charge will cause a quasi-uniform electric field between the barrier and the ground electrode, further increasing the withstand voltage [4]. For negative voltages the ionization takes place at the rod tip just as for the positive voltages. Electrons will move towards the ground electrode to the barrier leaving the heavier positive ions behind. This causes a *higher* electrical field. However, some distance from the tip of the rod the field strength is drastically reduced, hindering the ionization process of propagating further into the gap. The sum of these two opposite effects is a net increase in the breakdown voltage. Thus, it is explained that a space charge near the tip of the rod results in a field equalization in the region between the insulating barrier and the ground electrode [4].

According to [4], the withstand voltage can be increased up to three times the original value, for positive impulses, with the right barrier configuration. In [4] the optimal relation between the distance between the rod and the barrier and the distance between the rod and the ground electrode, ξ, is found to be 0.15-0.3. This optimal relation is also mentioned and supported by [13], [14] and [3]. For negative impulses the optimal relationship, ξ, has yielded an increase in withstand voltage by a factor of 0.3-0.5 [4].

2.5 Electric breakdown as a stochastic variable

The electrical breakdown of an insulation material is a stochastic process. The breakdown voltage will not be identical for each test instance. This is because the process is extremely sensitive to its initial conditions and random events. Such events are e.g. starting electrons and the collision of molecules.

Knowing the highest voltage that can be applied without running the risk of breakdown is important. However these low probability values are very difficult to determine experimentally. Therefore it is more practical to estimate the low probability values by extrapolating from know mathematical distributions [7]. One common and easy to estimate value is the value that results in a breakdown 50% of the time. This is the average value resulting in a breakdown $\bar{U}$ often denoted U_{50}.

The most used probability distributions to treat stochastic breakdown phenomena are the normal (Gaussian) and the Weibull distributions. For measuring the withstand strength of insulation materials, the Gaussian distribution gives a suitable approximation about the 50% value. For small samples and samples with high or low probability (tail values) the Weibull distribution is better suited. Here it is assumed that the experiments follow a Gaussian distribution.

Gauss distribution function:

$$P(U) = \frac{1}{\sigma\sqrt{2\pi}} \int_{-\infty}^{U} e^{(-\frac{1}{2})(\frac{U-\bar{U}}{\sigma})^2} dU \tag{2.8}$$

Standard deviation:

$$\sigma = \sqrt{\frac{1}{n-1} \sum_{i=1}^{\infty} (U_i - \bar{U})^2} \tag{2.9}$$

The true sample variance σ can only be obtained by an infinite number of tests. Therefore an estimator of the true variance, s, can be calculated from formulas 2.10 and 2.11. [13]

$$s^2_{up-down} = \frac{1}{n-1} \left\{ \sum_{i=1}^{n} U_i^2 - \frac{1}{n} (\sum_{i=1}^{n} U_i)^2 \right\} \tag{2.10}$$

$$s = 1.62\Delta U \left\{ \frac{s^2_{up-down}}{\Delta U^2} + 0.029 \right\} \tag{2.11}$$

2.5.1 Linear regression

Linear regression is often used on data sets in order to show trends in the data values. A commonly used method to calculate the linear trend is the method of least squares. The true linear trend, Y, can be calculated from equation 2.12 where ϵ represents the random error.

$$Y = \alpha + \beta x + \epsilon \tag{2.12}$$

An estimation of the true line, $\hat{y}(x)$ can be done by calculating the estimators a and b. This can be seen in equations 2.13, 2.14 and 2.15. Here $\bar{y}$ and $\bar{x}$ are the mean values of the measurements.

$$\hat{y} = a + bx \tag{2.13}$$

$$b = \frac{\sum_{i=1}^{n} (x_i - \bar{x})(y_i - \bar{y})}{\sum_{i=1}^{n} (x_i - \bar{x})^2} \tag{2.14}$$

$$a = \bar{y} - b\bar{x} \tag{2.15}$$

2.5.2 Breakdown and withstand voltage

In this thesis two values will be discussed, namely the breakdown voltage, $U_{BD} = U_{50}$, and the withstand voltage $U_{WS} = U_{02}$. The breakdown voltage has been defined earlier as the voltage that 50% of times will result in an electric breakdown. The withstand voltage on the other hand is the voltage level that will result in electric breakdown only 2% of the time and is the more relevant value when equipment

thresholds is considered. The withstand voltage is the breakdown voltage minus two times the standard deviation, which can be seen in Equation 2.16, [3].

$$U_{WS} = U_{BD} - 2 \cdot \sigma \tag{2.16}$$

Chapter 3

Method

3.1 Experimental set-up

3.1.1 Impulse voltage generator

The generator used in this project thesis is located at the high voltage laboratory E-152 at NTNU. The generator provides a controlled lightning impulse by coupling five impulse capacitors in series when triggered. The main components of the generator are:

- Control desk where the charging voltage and the sphere gap voltage is adjusted
- Transformer used to charge the impulse capacitors
- Rectifier to rectify the charging voltage
- Five impulse capacitors
- Five sphere gaps used to couple the capacitors in series
- Discharge capacitor

The symbols in figure 3.1 are explained in table 3.1 along with the associated values.

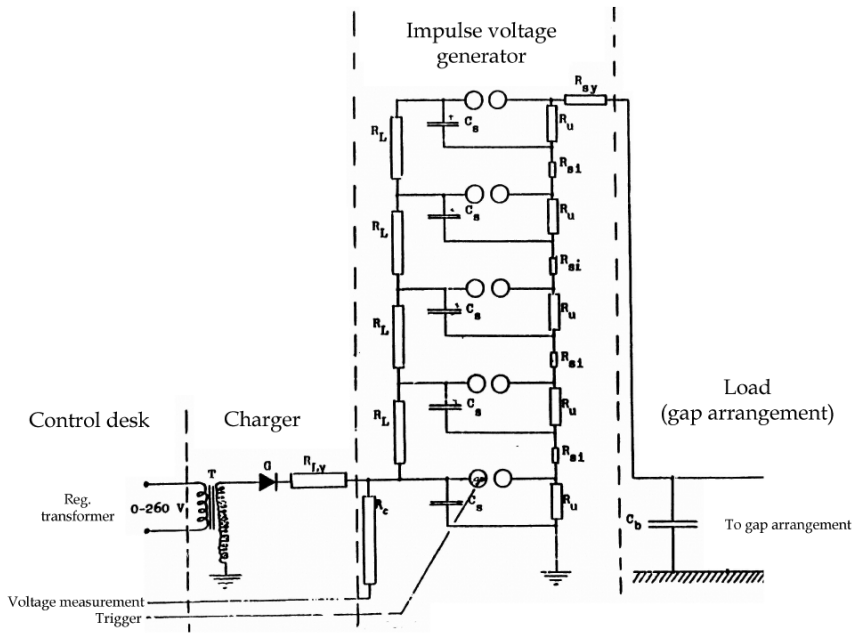

Figure 3.1: Circuit drawing of the impulse generator used to apply impulses to the test object. The most important components are the high voltage transformer, the charging capacitors, and the sphere gaps. The symbols in the drawing are explained in table 3.1. [2]

Table 3.1: The component names and values of impulse generator as seen in figure 3.1 [2].

Symbol	Component	Value
T	Transformer	-
G	Rectifier	-
R_{Ly}	Charging resistor	$1M\Omega$
R_F	Measuring resistor	$160M\Omega$
R_L	Charging resistor	$30k\Omega$
R_u	Discharge resistor	326Ω
R_{si}	Series resistor	55Ω
R_{sy}	Series resistor	570Ω
C_s	Discharge capacitor	$0.25\mu F$
C_b	Discharge capacitor	$560pF$

The IEC 61180 standard that concerns high voltage testing calls for a 1.2/50 voltage impulse. This means a rising time of 1.2 μs and a 50 μs duration to the half value of the voltage. A sample of the impulse can be seen in figure 3.2. The rise time is

1.42 μs which is within the limit of 1.2 $\mu s \pm 0.36 \mu s$ set by the IEC61180 standard. The time to half the value was roughly measured to 48 μs.

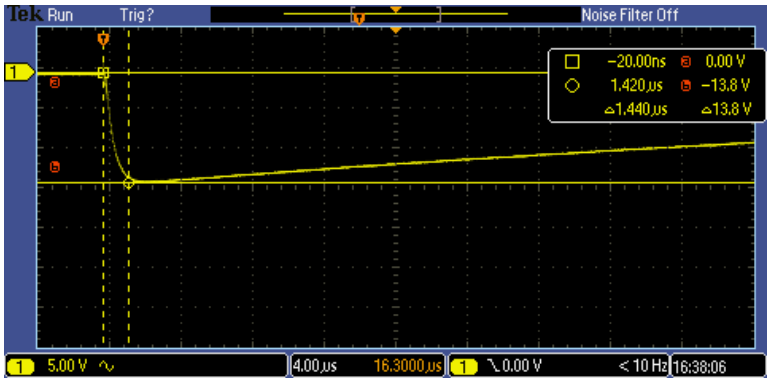

(a) Sample negative impulse without an electrical breakdown.

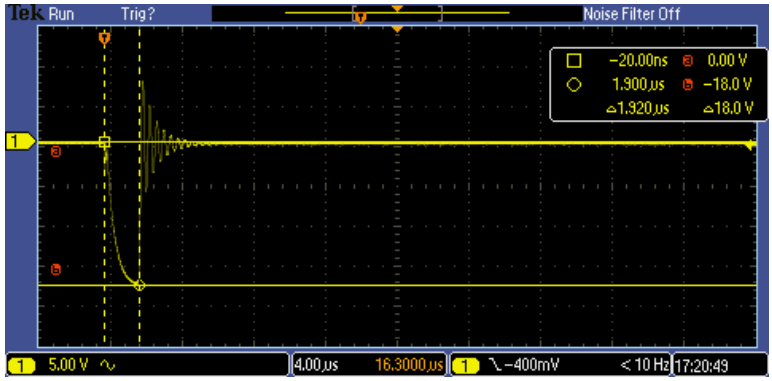

(b) Sample negative impulse with an electrical breakdown.

Figure 3.2: Captured images from the oscilloscope showing a test with and without electrical breakdown respectively. The signal amplitudes and rise times are measured with the cursor measuring device. The polarity of the impulses are arbitrary, the figure is only meant to illustrate the measurement of amplitude and rise times.

3.1.2 Measuring equipment

Voltage impulse measurements were done with a Tektronix MSO2024B Mixed Signal Oscilloscope. Whether an impulse lead to a discharge or not, a large enough surface charge to saturate the voltmeter could be measured on the barrier. This surface charge would severely affect the test results and had to be removed. The barrier was therefore cleaned of residual charge with a cloth laced with isopropyl

alcohol (2-propanol) between each impulse. A TRek model 520 electrostatic voltmeter was used in order to ensure there was no significant residual charge left on the barrier.

3.1.3 Measuring circuit

In order to correctly measure the impulse voltages a measuring circuit was coupled between the impulse generator and the oscilloscope, after the "To gap arrangement" node in figure 3.1. This measuring circuit can be seen in figure 3.3. The circuit consists of several voltage dividers in order to avoid the large applied voltages directly on the oscilloscope. The impedance and resistive values are respectively:

- $R_1 = 10\ k\Omega$
- $R_2 = 12.5\ \Omega$
- $Z_k = 50\ \Omega$ characteristic impedance
- $R_3 = 40\ \Omega$
- $R_4 = 10\ \Omega$

The relation between the measured voltage and the voltage impulse applied can be calculated as shown in equations 3.1 and 3.2.

$$U' = U_{generator} \cdot \frac{R_2 \parallel Z_k}{R_1 + R_2 \parallel Z_k} \tag{3.1}$$

$$U_{scope} = U' \cdot \frac{R_4}{R_3 + R_4} = U_{generator} \cdot \frac{R_2 \parallel Z_k}{R_1 + R_2 \parallel Z_k} \cdot \frac{R_4}{R_3 + R_4} \tag{3.2}$$

Inserting values into equation 3.2 gives the following relation seen in equation 3.3.

$$U_{generator} = 5005 \cdot U_{scope} \tag{3.3}$$

These equations may seem contrary to classical circuit analysis. However they deal with a travelling wave moving from the generator side to the scope side. The travelling wave only "sees" the first impedance it encounters on its way (Z_k). This wave also has to be terminated, which is the reason the sum of R_3 and R_4 equals the impedance value of Z_k. The wave energy is then absorbed by R_3 and R_4 and no reflection takes place [15].

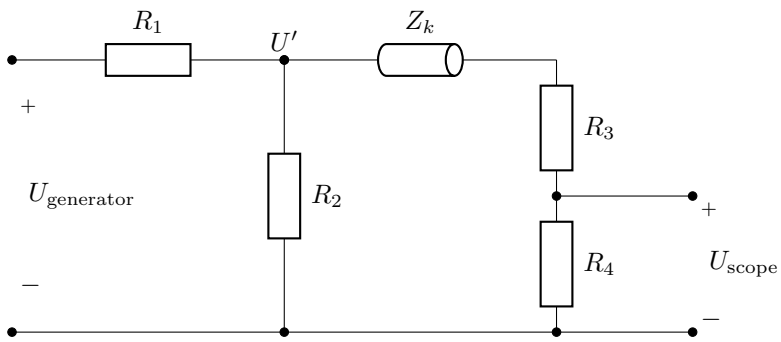

Figure 3.3: Measuring circuit placed between the impulse generator and oscilloscope. The circuit is a series of voltage dividers in order to avoid large voltages from the impulse generator directly on the scope. The wave impedance Z_k is the characteristic impedance of the cable to the oscilloscope.

3.1.4 Photography

The streamer path was captured with a camera. To document the actual streamer path at breakdown, the control desk was set to trigger manually. A single-lens reflex camera with a shutter time of $1.3s$ was then used take a photography of the streamer. The camera used was a Nikon D80 with a Sigma 18-50mm f/2.8 EX lens.

3.1.5 Gap arrangement

The tests were done with a customized arrangement made from drawings from Solbakken [3], and built by the workshop at the Department of Electric Power Engineering.

The rig used for the experiments comprised of a high voltage electrode, ground electrode, barriers, and a support system for the barriers. The high voltage electrode was a rod with a diameter of 7 mm and a spherical tip with the same diameter. The rod was held in place by an adjustable clamp and a wooden support frame. A plate made of steel and aluminium formed the base of the rig. This plate was grounded and served as the ground electrode. The relevant dimensions and names are seen in figure 2.2.

The barrier plates were held in place by two sets of polycarbonate supports. The supports had slits in them in order to facilitate different barrier heights. The barrier plates were fashioned out of another polycarbonate material (Lexan). The plates measured 600 mm × 600 mm. To give additional mechanical support the plates were held up by pieces of Lexan at the edges of the plates far enough out to not disturb the electrical field. The dimensions of the rod, barriers and arrangement can be seen in figure 3.4. In figure 3.4 the barriers are shown to have a thickness of 5 mm. The barriers in this thesis however are kept at a thickness of 1 mm.

Due to the limitations of the impulse generator the gap distances and protrusions in this thesis were limited to a minimum of 20 mm and a maximum of 60 mm. For gap distances below 20 mm the positive impulse became close to impossible to fire due to the low distance required between the sphere gaps of the five discharge capacitors. The typical result of such a failed attempt, was a flash over between one of the five pairs which gave a discharge impulse of $\frac{1}{5}$ of the desired impulse magnitude. When firing the negative impulses the limitation was somewhere above a gap distance of 60 mm due to the high corona activity in the sphere gaps.

The gap distances were adjusted using metal cylinders made in the workshop cut with a precise height in order to give consistent values.

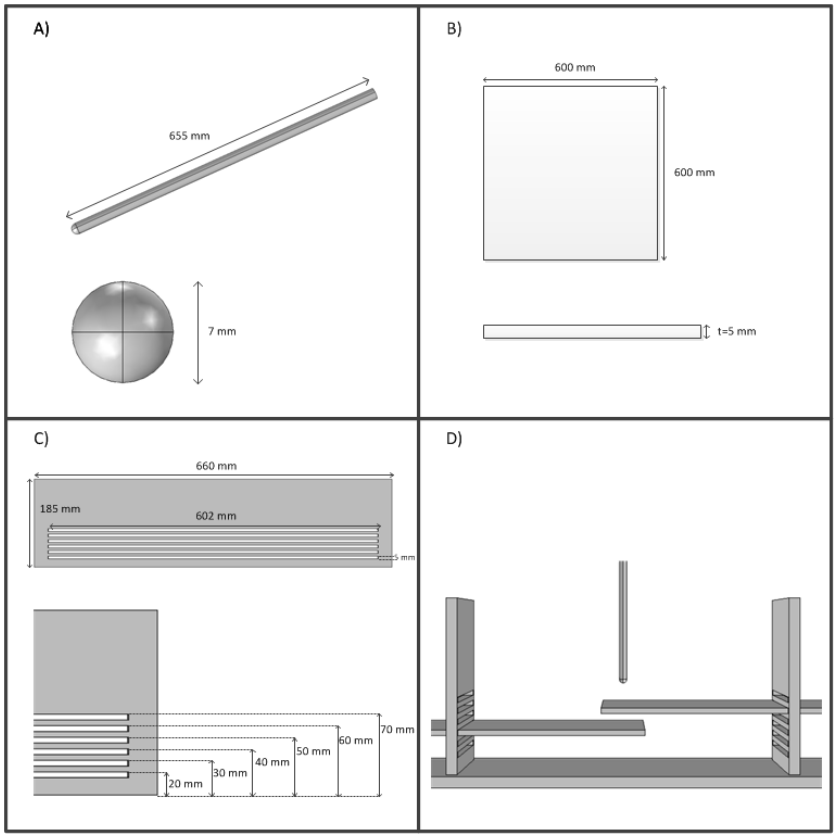

Figure 3.4: Test arrangement. A) Shows the rod length and diameter. B) Shows the length, width and thickness of the barriers. NB: The thickness of the barriers used in most of the tests in this thesis is 1 mm. C) Shows the barrier support system and dimensions. D) Shows the mounted test arrangement. [3]

3.2 Experimental method

3.2.1 The up-and-down method

The up-and-down method is widely used to estimate the 50% probability of the breakdown voltage U_{50} also called U_{BD}. The method is as follows: A voltage impulse U_n, in the region of the true breakdown voltage is chosen. The impulse voltage is then applied. The result, whether it yields a breakdown or not, is recorded along with the voltage level. If the applied voltage results in a breakdown the voltage is reduced by a fixed value of ΔU. The result for the next voltage applied $U_{n+1} = U_n - \Delta U$ is then recorded in the same manner. Likewise if an applied voltage does not result in a breakdown, the next applied impulse voltage is then adjusted up: $U_{n+1} = U_n + \Delta U$. The IEC 60060-1 standard, concerning test methods for high voltage applications, requires a minimum of $n = 20$ total impulse applications in the relevant region in order to determine the 50% withstand voltage U_{50} [13]. This means the impulse applications spent searching for the breakdown region is omitted from the calculations. The best results of the up-and-down method are obtained when the voltage steps ΔU is close to the sample variance. An advantage of the up-and-down method is that it requires few applied impulses compared to other statistical methods to give the same level of statistical confidence.

In this experiment, the the smallest practical adjustment to the charging voltage was 0.5 kV. For the five charging capacitors this meant a total step of $\Delta U = 5 \cdot 0.5$ kV = 2.5 kV for each voltage adjustment. The results of the test were saved in an Excel spreadsheet for later analysis. The linear regression explained in section 2.5.1 was obtained by importing the excel sheet to a Matlab script. When the data is collected from the valid breakdown region, the mean of the sampled voltages is the 50% breakdown voltage U_{50} [3]. A conceptual example of a test done with the up-and down method can be seen in figure 3.5.

When choosing ΔU, there are some dangers related to picking either a value that is too small or one that is too big. If the ΔU is too big, the true voltage interval of the 50% value will be "circled" in too wide a band, which would lead to inaccurate results of the measurements. Should ΔU be given too small a value on the other hand, there is a risk that the ramping up will be included in the mean calculations (as there is always a chance that breakdown will occur during ramping). Thus ending the test too early. If this is the case, the calculated 50% value will be too small compared with the real 50% value. One way to avoid the problem with a too small ΔU is to register several of the impulses and resulting breakdown or no breakdown. Then, the results that are included in the mean can be more carefully chosen so that the test is not ended prematurely.

Standard deviations for these types of experiments are always difficult to control. To ensure the quality of the experimental work, all tests with a standard deviation above 4 kV were re-done until a lower standard deviation was achieved.

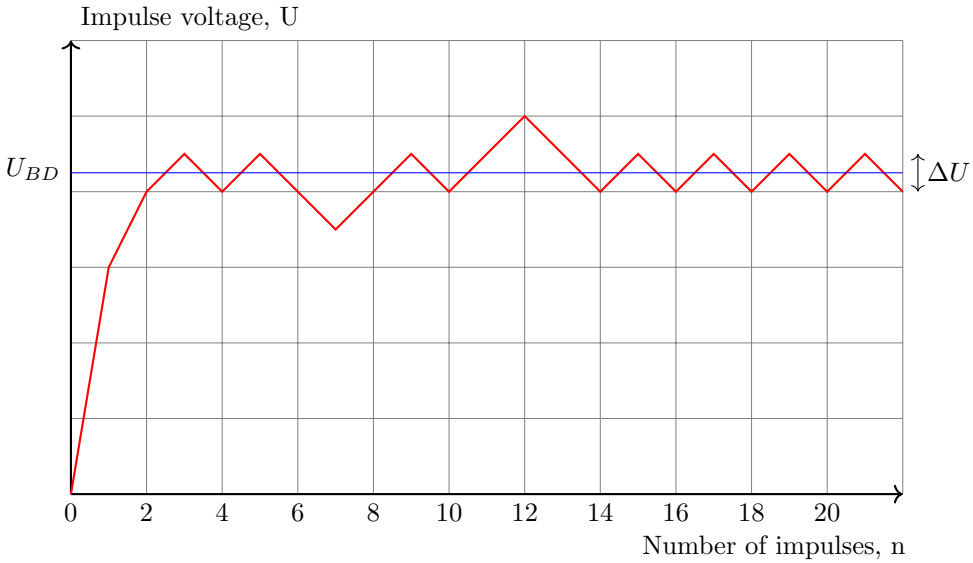

Figure 3.5: A conceptual example of a test done with the up-and down method. The impulse voltage is adjusted up or down by ΔU depends on whether the impulse results in a breakdown or not. The blue line marks the average of the breakdown voltages in the valid area (the ramping up is not included).

3.2.2 Barrier charge measurements

In order to quantify the charge on a barrier after an impulse, an electrostatic discharge monitoring system was used to measure electric field strength. The system measures electric field strength in $[\frac{kV}{meter}]$. This monitoring system consists of a measuring probe and a monitor. The component models and serial numbers can be seen in appendix A. The measurements were conducted in a time series of 170 minutes, after which it was assumed the charge decay entered a linear development. The first measurement was read 5 minutes after the impulse was fired. The reason for the 5 minute delay was the amount of time it took in order to mount and calibrate the measuring probe. The calibration was done by mounting the probe above the ground electrode, and adjusting the panel output to 0 $\frac{kV}{meter}$. Then, the probe replaced the high voltage rod in the mounting, at a distance of 100 mm from the top of the barrier. These measurements were conducted for both impulses that did, and did not result in electrical breakdown.

3.2.3 Correcting for air density

Electrical breakdown is a function of the air density and temperature. The measured breakdown voltage U_0 is corrected for air pressure according to equation 3.4. Air pressure and temperature was measured by a small wireless weather station placed in the lab and used for the measurement results. The air density correction factor, k_1 depends on the relative air density, δ. k_1 can generally be expressed as $k_1 = \delta$ [7]. In Equation 3.5 p is the measured pressure, $p_0 = 1013$ hPa - the standard pressure (approximately one atmosphere), t is the ambient measured temperature, and $t_0 = 20$ is the standard reference temperature in degrees Celsius.

$$U = k_1 \cdot U_0 \tag{3.4}$$

$$\delta = \frac{p}{p_0} \cdot \frac{273 + t_0}{273 + t} \tag{3.5}$$

3.3 Field distribution calculations

To predict the streamer inception and propagation it is important to know the electric field distribution. This field distribution can be calculated by FEM software programs such as e.g. COMSOL Multiphysics. By using COMSOL geometries, boundary conditions and material properties can be defined. COMSOL can then compute the Laplacian equations and return the electric field distribution in the model.

3.3.1 COMSOL model properties

The rod in the model is a cylinder with a spherical tip that is excluded from the model. The electric field strength in the high voltage electrode is $0\frac{kV}{mm}$, so the exclusion from the model will satisfy this requirement. The exclusion of the rod from the model also ensures the rod is just a boundary surface with a potential in the simulations. This avoids problems with boundary conditions and material properties. COMSOL will take the mean of the values in two materials when computing values in the boundary between the two materials, which is a slight source of error in COMSOL. The same choice is done with the grounding plate which is also the bottom boundary surface of the model assigned ground potential. The insulating barrier is made of "Acrylic plastic", a predefined material in COMSOL. The relative permittivity of the barrier, ε_r, was set to 2.3.

The electric field for the rod-plane gap has been calculated using COMSOL 5.2. For easier configurations the physical dimensions of the model is been parametrised. This allows for easy adjustments of barrier positions and the number of barriers and adjusting the rod-plane distance as well as barrier heights. The model can be seen in figure 3.6. The depth is 300 mm, the height is 200 mm and the length is 600 mm.

The model was built in three dimensions and the depth symmetry was exploited to allow for a more compact model, reducing the computational stress. The majority of the model was meshed in a "fine" grade mesh. However, this was not sufficient for the region around the tip of the rod. In this region a free tetrahedral partition with a finer mesh was applied. The rod was given electric potential and the bottom electrode was assigned ground potential. The "roof", "walls" of the model and the barriers were assigned charge conservation. The model domain is a rectangular box, seen in figure 3.6, where two of the walls along with the roof is hidden from view.

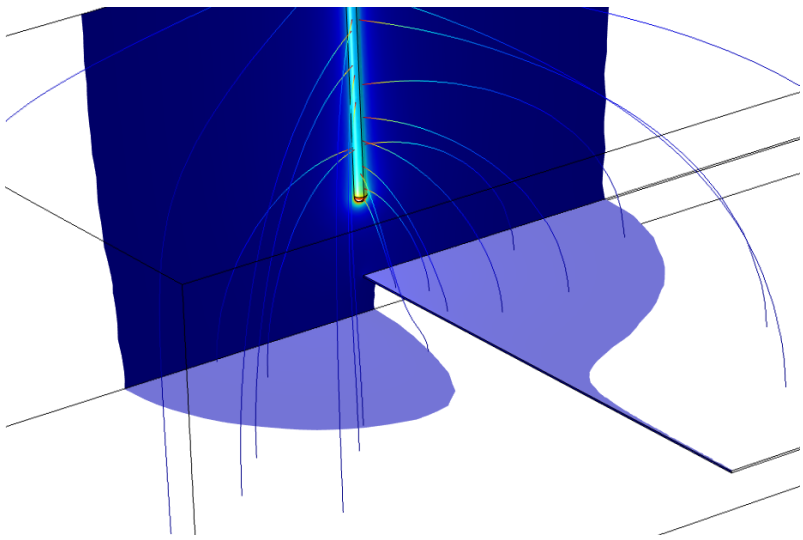

Figure 3.6: Geometry of the COMSOL model. The high voltage rod is highlighted and cut in two by the mirroring surface. Below the rod is the insulating barrier, protruding 0 mm from the centre of the rod. The blue shaded area shows the regions of the model where the electric field exceeds 0.54 $\frac{kV}{mm}$ for an arbitrary rod voltage. The coloured lines are the electric field lines and the colour grading signifies the magnitude of the electric field.

3.3.2 Parameter sweeps

One parameter of interest when investigating breakdown voltage, is the amount of charge deposited on the barrier during the impulse. High speed photographs of impulses suggest a considerable accumulation of charge on the top and on the side edge of the barrier [16]. To simulate this, a charge potential was applied to the top and the side edge of the barrier in the COMSOL model. The charge was modeled as evenly distributed electric potential. In order to evaluate the amount of charge on the barrier, a so called "parametric sweep" was conducted for all the different configurations. In this sweeping process the goal was to determine the

charge required to achieve a contiguous electric field with a higher, or equal to, strength than 0.54 $\frac{kV}{mm}$, which is the field strength required for a self propagating streamer under impulse conditions [1].

3.4 Streamer inception voltage calculation

When the electrical field distribution is known, it is possible to extract this information and use it to calculate the streamer inception voltage. By using a script in e.g. Matlab the value of α_{eff} in equation 2.3 can be calculated in discrete steps. The integral can then be solved with respect to $ln(N_c)$.

The streamer inception voltage calculation script in this thesis, seen in appendix B, is based on a script by Atle Pedersen, Research Manager at SINTEF Energy Research. The original script was made to calculate inception voltage in a barrierless gap. The ionization coefficients are found in [12]. The original script was also adapted to a 2D field simulation, so there are some modifications done to accommodate the 3D field line matrix extracted from COMSOL in this thesis.

The calculations are divided in several steps. The first point is to extract the data of a field line seen in figure 3.6. The simulation is based on a primary case where the voltage applied to the rod is 1 kV. It is assumed that the field distribution itself is solely a function of the geometry of the figure. The extracted data matrix from COMSOL contains the three positions in x- y- and z- directions,(which gives the integration path Γ, following the field line), the electric field strength in all the points, along with one column with the number of the field line. In these simulations, 200 field lines were generated in COMSOL and then sorted in MATLAB. The field lines were all generated from the rod. Most of the field lines were aroubd the tip of the rod, and some were generated higher up on the rod.

The sorting function goes through all the 200 extracted field lines and picks the line with the strongest field at the beginning of the line. It is assumed that this is the line where streamer inception will occur with the lowest applied rod voltage. Once the most critical field line is found, a new, higher voltage, is applied and the field strength is scaled in a separate function. When the field is scaled, the field line is integrated according to equation 2.3. If the streamer inception criterion is satisfied, the function returns the applied voltage that satisfied the criterion. If the integration does not accumulate the required amount of electrons, the process is repeated until streamer inception occurs. It is worth noting that the function only takes into account the electrons that are generated at the tip of the rod. Field strength simulations show that the electric field may become stronger along the length of the line and thus contribute to electron accumulation further along the integration path. The integration function aborts in the first step where the electric field strength no longer contributes to the accumulation of electrons.

Chapter 4

Results and Discussion

4.1 Experimental lab results

These are the results of the experiments to determine the withstand voltage in the high voltage lab. The withstand and breakdown voltage measurements were conducted for a series of barrier configurations by using the up- and down method. Gap distance between the high voltage rod and the ground electrode was kept constant at 60 mm for all of the tests. The results are summed up in table 4.1, where breakdown and withstand voltage can be seen, along with the standard deviation. The development of the withstand voltage in the different configurations can be seen in figure 4.1.

4.1.1 Breakdown voltage measurements

Figure 4.2 shows the development of the breakdown and withstand voltages as the barrier was lifted from 20 mm to 60 mm in increments of 10 mm. The barrier protrusion in figure 4.2 is kept constant at 0 mm. One result of particular interest from these tests is that the breakdown voltage is increased by 10% when the barrier is lifted from 20 mm to 30 mm from the ground electrode. Possible explanations for this result is further discussed in section 4.2.

Figure 4.3 shows the breakdown and withstand voltages for configurations with a barrier protrusion kept at a constant 40 mm. In this figure a gradual increase can be seen when the barrier is lifted. The breakdown voltage decreases again when the barrier touches the rod and $d = 60$ mm. This is expected and further discussed in section 4.2.

Figure 4.4 shows the development of the breakdown and withstand voltages as the barrier heights are kept constant and the protrusion is increased from 0 mm to 40 mm. In figure 4.4a the height is 30 mm and in figure 4.4b the barrier height is 50 mm. The results in this figure contradict the assumptions made in section 2.3.1 and equation 2.7. In section 2.3.1 it is assumed that a prediction can be made

based on the withstand voltage in a barrier-less gap and the internal streamer field strength. Figure 4.4a shows that the shortest path x_s is not directly a parameter of the breakdown voltage when the barrier height is 30 mm. For the configurations with a barrier height of 50 mm however, the protrusion directly influences the breakdown voltage, as seen in figure 4.4b.

All configurations perform their worst when the barrier is touching the rod. This is because the barrier then works as an extension of the rod and thus strengthening the electric field. For the case of the 0 mm protrusions this configuration reduces the withstand voltage with 18%. This can be explained by a strong tangential field allowing the streamer to propagate along the surface of the barrier. For the 0 mm barrier protrusions the configuration with the highest withstand voltage improvement was with a 30 mm barrier height. For the 20 mm protrusion, the best performance is at 30 mm barrier height. For 40 mm protrusions the best performance is at 50 mm barrier height. The 20 mm protrusions are outperformed or performs equally to the other two configurations of 0 and 40 mm as seen in table 4.2.

Table 4.1: Measured withstand voltage, U_{WS}, breakdown voltage, U_{BD}, and standard deviation, σ, for impulses with barriers protruding 0, 20 and 40 mm from the centre of the rod.

d [mm]	0 mm protrusion			20 mm protrusion			40 mm protrusion		
	U_{WS} $[kV]$	U_{BD} $[kV]$	σ $[kV]$	U_{WS} $[kV]$	U_{BD} $[kV]$	σ $[kV]$	U_{WS} $[kV]$	U_{BD} $[kV]$	σ $[kV]$
20	71.1	75.6	2.27	81.0	84.0	1.48	79.4	82.6	1.61
30	81.9	85.6	1.82	77.4	82.6	2.61	79.5	84.5	2.48
40	75.9	81.7	2.90	81.9	87.5	2.82	84.7	88.4	1.84
50	73.8	81.0	3.60	76.8	84.5	3.82	87.5	92.5	2.50
60	53.5	58.7	2.60	67.5	71.7	2.06	79.5	84.5	2.48

Table 4.2: Improvement to withstand voltage in comparison to the withstand voltage in a barrier-less gap. The barrier thickness for all instances is 1 mm.

Barrier height, d	Improvement in withstand voltage[%]		
	p = 0 mm	p = 20 mm	p = 40 mm
20 mm	10.9	21.9	20.3
30 mm	22.7	18.2	20.4
40 mm	16.6	22.7	25.3
50 mm	14.2	17.6	27.6
60 mm	-18.3	6.3	20.4

Evaluation of the breakdown voltage prediction

Based on the reference value of the breakdown voltage in the barrier gap, a calculation was made from equation 2.7 and the shortest path (b) in figure 2.3. The result can be seen in table 4.3. These results show that equation 2.7 proposed

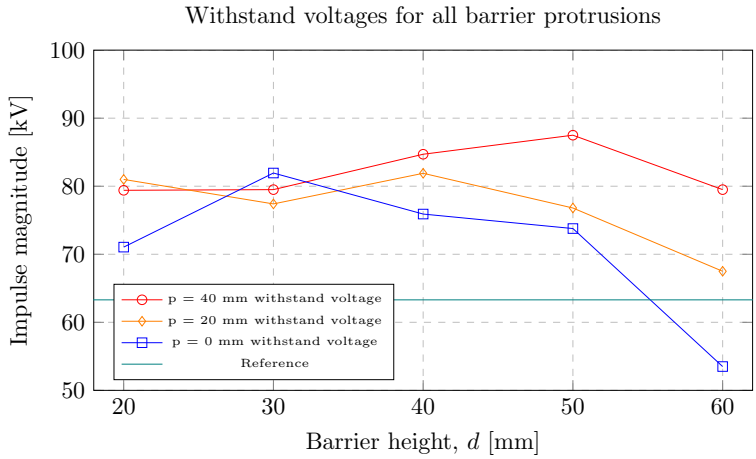

Figure 4.1: Withstand voltages for all the configurations with 1 mm barrier thickness. The reference is the withstand voltage in the gap without a barrier. The results can also be seen in table 4.1.

in section 2.3.1 gives a poor prediction of the breakdown voltage for some configurations. Especially in the configurations with the 0 mm barrier protrusion the prediction from Equation 2.7 fails completely. As the geometrical shortest path remains unchanged, the 0 mm protrusion set up is well suited to examine the other effects associated with the breakdown voltage. The results further strengthens the theory that the breakdown voltage is more affected by the barrier's influence on the field distribution, than the increasing length the streamers and leaders are forced to traverse towards the ground electrode. This is most significant for small barrier protrusions of 0-20 mm or 0 to 33% of the rod-plane gap distance.

By comparing the lengths of x_s for the different configurations in table 4.3 to figure 4.1, there is no general relation between the length of x_s and $U_W S$. The configurations with 0 and 20 mm protrusion show a tendency where $U_W S$ decreases with increasing x_s for some barrier settings. However, for the 40 mm protrusion the increased streamer path correlates with the change in withstand voltage. The highest improvement is seen to match the longest geometrical (shortest) distance (except where the rod touches the barrier). By comparing table 4.1 and table 4.3 the predictions from Equation 2.7 represent a conservative estimation (up to 10% higher than estimated) and could therefore be used in design processes.

4.1.2 Field strength measurements

To determine the magnitude of charge present on the barrier after an impulse the field strength was measured with a probe. The magnitude and decay over time can be seen in figure 4.5. These decay measurements were varying quite a lot in terms of charge magnitude, but the slope of the decay was fairly consistent. The

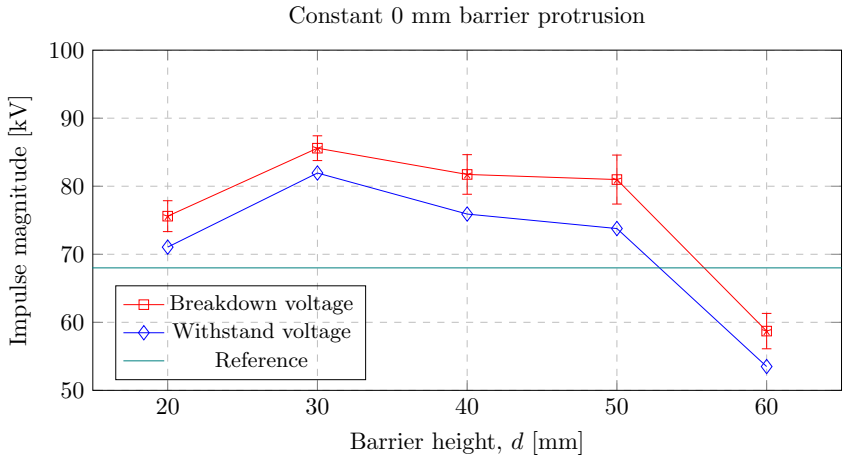

Figure 4.2: 0 mm barrier protrusion with measured breakdown and withstand voltages. The standard deviation is shown in the vertical error bars. The reference is the breakdown voltage in the gap without a barrier. The results can also be seen in table 4.1. The barrier thickness is 1 mm.

Table 4.3: The shortest streamer path x_s calculated from Equation 2.6, predicted withstand voltage, U_{pred}, calculated from Equation 2.7 and the fault of the prediction compared to the measured results in per cent. Negative faults predicated too high a withstand voltage.

d [mm]	0 mm protrusion			20 mm protrusion			40 mm protrusion		
	$x_s[mm]$	$U_{pred}[kV]$	Fault [%]	$x_s[mm]$	$U_{pred}[kV]$	Fault [%]	$x_s[mm]$	$U_{pred}[kV]$	Fault [%]
20			12.3	64.7	65.9	18.6	76.6	72.3	9.82
30			29.4	66.1	66.7	14.0	80.0	74.1	7.29
40	60.0	63.3	19.9	68.3	67.8	17.2	84.7	76.7	10.4
50			16.6	72.4	70.0	8.85	91.2	80.2	9.10
60			-15.5	80.0	74.1	-9.78	100	84.9	-6.36

average decay slope was calculated to be $-0.14078 \cdot \frac{kV}{meter}$ per minute. On average, the impulses that resulted in breakdown deposited about 40 % of the charge that was deposited when there was a breakdown. For other materials than Lexan, one method of cleaning the barrier of charge was simply to fire an impulse that resulted in flash over. As can be seen in figure 4.5 this is not a satisfactory cleaning procedure with Lexan plates.

The measuring probe also made it possible to more precisely evaluate the efficacy of the isopropyl cleaning of the barriers. Using the field strength measuring probe on the plate after washing, it was clear that not all the charge was removed. The measurements showed that a minimum of about 3 $\frac{kV}{meter}$ and a maximum of 9.9 $\frac{kV}{meter}$ was left on the barrier after a cleaning. This translates to 300 V and 990 V respectively. Here it is assumed that the electric field is can be translated

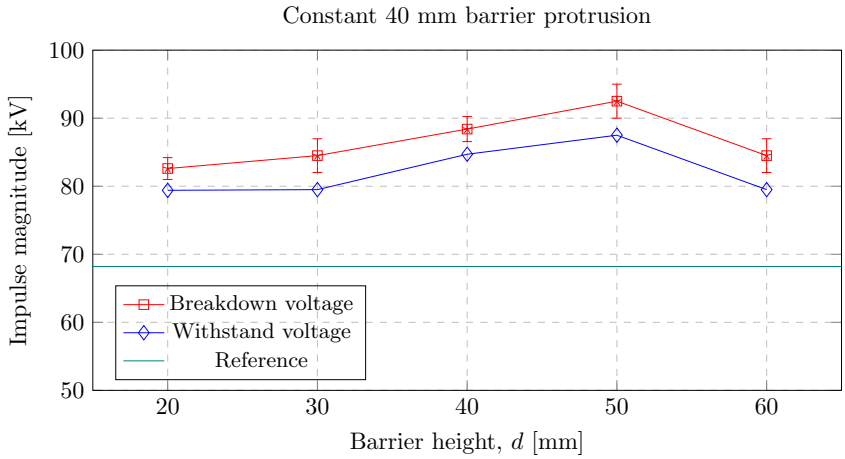

Figure 4.3: 40 mm barrier protrusion with measured breakdown and withstand voltages. The standard deviation is shown in the vertical error bars. The reference is the breakdown voltage in the gap without a barrier. The results can also be seen in table 4.1. The thickness of the barrier is 1 mm.

directly to voltage potential by multiplying with the distance (although it is also a function of the charge distribution on the barrier).

It is important to note that the measurements shown in figure 4.5 are the sums of all the contributions from the charge carriers on the barrier to the electric field strength. These results are not directly transferable to charge density or voltage. The field strength measurements contain no information the distribution of the charges. Thus the observed decay may not be charge carriers leaving the barrier, but simply charge distributing evenly on the surface of the barrier. By setting 0.115 $\frac{kV}{meter}$ as the new data range in COMSOL, a parametric sweep was conducted to determine the required voltage applied to the barrier in order to achieve the measured voltage at 100 mm from the barrier. The sweep showed that the required voltage applied was somewhere between 37 kV and 38 kV. To achieve the field strength measured on the barrier when there was no breakdown, 0.043 $\frac{kV}{mm}$ at 100 mm distance, the calculations in COMSOL gave a voltage potential on the barrier of between 14 and 15 kV. Again, this is the maximum field strength measured five minutes after the impulse, and the voltage on the barrier in the COMSOL model is evenly distributed. The field distribution calculations can be seen in appendix D, figures D.1 and D.2 respectively.

4.1.3 Streamer paths at breakdown.

To verify the assumptions on the actual path of the streamer at breakdown, photographs were taken of the flash over sparks. The pictures confirm that the streamer path follows all the paths shown in figure 2.3. The pictures were taken for the

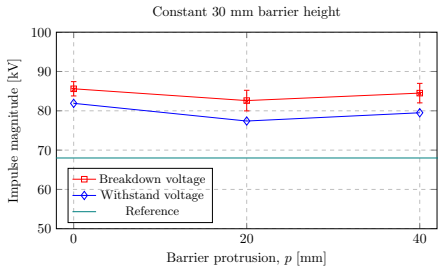

(a) Constant 30 mm barrier height with measured breakdown and withstand voltages.

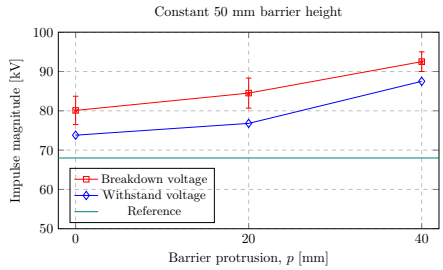

(b) Constant 50 mm barrier height with measured breakdown and withstand voltages.

Figure 4.4: Withstand and breakdown voltages for constant barrier heights of 30 and 50 mm with varying protrusions The barrier thickness is 1 mm. The standard deviation is shown in the vertical error bars. The reference is the breakdown voltage in the gap without a barrier. The results can also be seen in table 4.1.

project thesis leading up to this master's thesis, and the configurations differ slightly from the configurations used in this thesis. The pictures can be seen in appendix E. What can be observed is that the streamer at breakdown follows what seems to look like "path c" in figure 2.3 when the barrier is far from the high voltage rod. When the barrier is closer to the rod, the plasma channel seems to follow what is closer to the shortest path x_s. This may explain why the predicted voltages in table 4.3 tend more toward the observed voltage as the barrier is moved closer to the high voltage rod.

4.2 Field distribution calculations

Conducting parametric sweeps is a way of simulating the charge accumulation on the barriers with very simple tools. The work behind the paper written by Meyer et al. ([16]) was conducted simultaneously with this thesis. This paper features high speed pictures of streamer inception and propagation on the same experimental test set up as this thesis. The pictures of the streamers show how charge accumulates on the top and on the sides of the barriers. This charge accumulation is one of the more important effects when it comes to barriers' ability to increase withstand voltage. The field distribution calculations show how the charge helps negate the electric field and lower the field strength between the barrier and the high voltage rod for the 40 mm protruding barrier.

Figures 4.7 and 4.6 show two of the results of the parametric sweeps conducted in COMSOL. Here the barrier charge was simulated by applying an electric potential directly to the barrier top and side. By examining figures 4.6a to 4.6d it can be seen that the barrier requires a charge of around 34 kV in order to obtain an electrical field in which the streamer can self-propagate down to the ground electrode

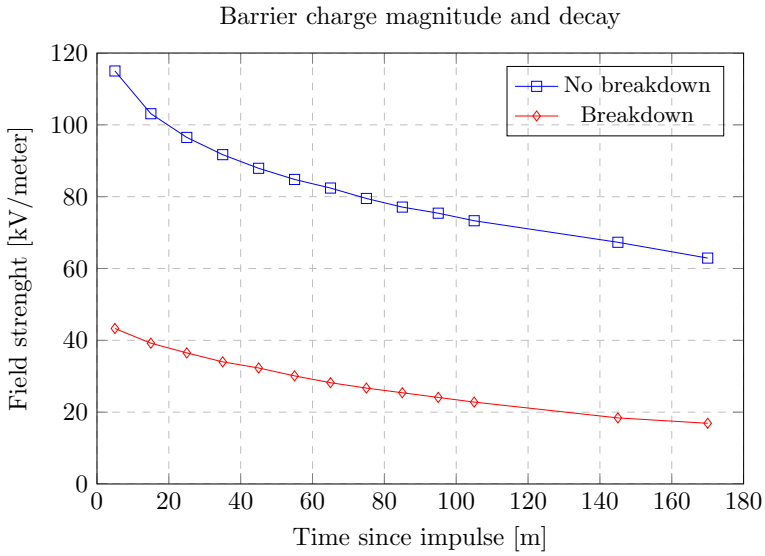

Figure 4.5: Measured field strength on the barrier after an impulse. The graph shows the charge magnitude over time on the barrier, with and without a breakdown respectively. The measuring probe was placed 100 mm above the barrier and directly above the tip of the rod.

for the 30 mm barrier height. For the 20 mm barrier height, only a 24 kV charge is required in order to obtain a field in which the streamer can self propagate towards ground.

Table 4.4 shows the required voltage applied to the barrier that gives a contiguous electrical field with field strength $E_{norm} \geq 0.54 \frac{kV}{mm}$. Note that the configuration where the barrier is at 60 mm and touches the rod is excluded. The calculations collapse as the barrier touches the rod and the calculated field strength is $E_{norm} \geq 0.54 \frac{kV}{mm}$ for the entire domain of the model. These simulations show an increase in the required barrier charge for the 0 and 20 mm barrier protrusion as the barrier height increases. The longer distance between the ground and the barrier means a higher charge is necessary for the field to bridge the gap between the barrier and the ground. The increase in the required voltage does not directly signify an increase in the withstand voltage, as seen in table 4.1. Here, a more complex relationship between the electric field from the rod voltage and the electric field from the charge deposited on the barrier is in play. The 40 mm barrier protrusions show a decrease from 20 to 40 mm barrier height, and then an increase again as the barrier height reaches 50 mm.

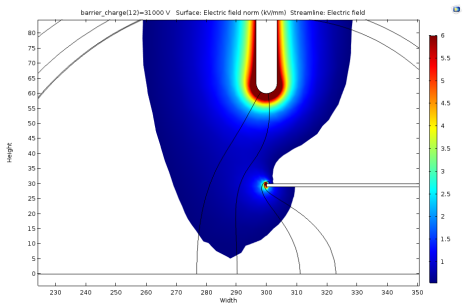

(a) Applied voltage to the barrier is 31 kV.

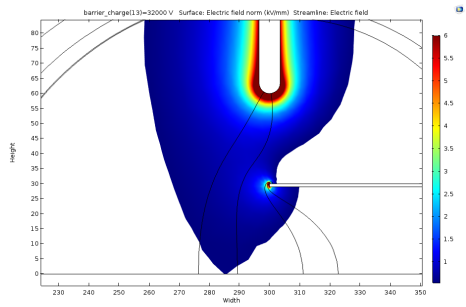

(b) Applied voltage to the barrier is 32 kV.

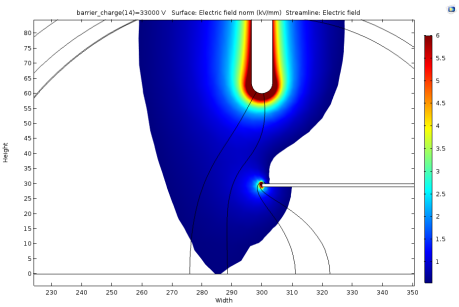

(c) Applied voltage to the barrier is 33 kV.

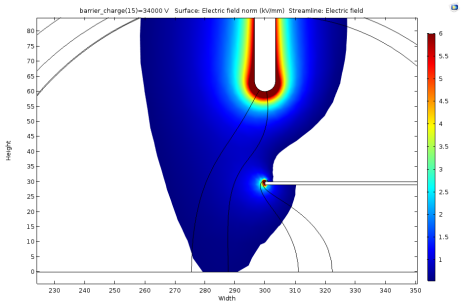

(d) Applied voltage to the barrier is 34 kV.

Figure 4.6: Field distributions with applied breakdown voltage U_{BD} on the rod. The white area signifies the region where the electric field $E_{norm} \geq 0.54\ \frac{kV}{mm}$. The color code ranges 0.54 (dark blue) to 6 from $\frac{kV}{mm}$ (dark red). Figures (a) to (d) show applied rod voltage $U_{BD} = 85$ kV, barrier height $d = 30$ mm, barrier protrusion $p = 0$ mm, barrier thickness, $t = 1$ mm.

4.3 Inception voltage calculations

Figure 4.8 and table 4.5 show some of the results of the inception voltage calculations. These results suggest that the background field is to some degree affected by the presence of the barrier and that this effect is again enough to affect the streamer inception voltage. The configurations with the barrier height at 20 mm have a similar inception voltage. This might signify that the field "distortion" or enhancement at the edge of the barrier is too far away to affect the inception voltage, which is mostly concerned with the area around the tip of the rod. Figure C.1 shows the electric field strength as a function of the length of the field line. This figure shows that the field strength drops lower than the threshold of the α integration of about 2.6 $\frac{kV}{mm}$. In this case the actual integrated length of the final field line

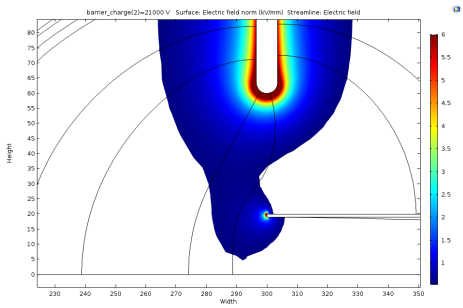

(a) Applied voltage to the barrier is 21 kV.

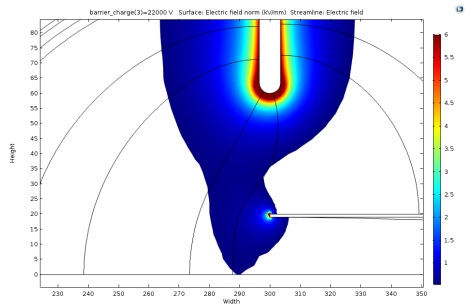

(b) Applied voltage to the barrier is 22 kV.

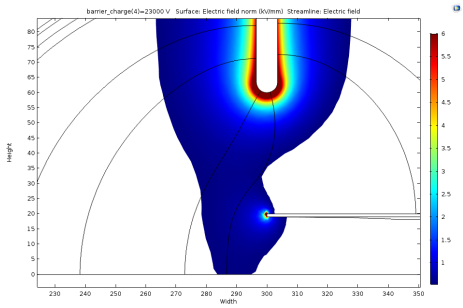

(c) Applied voltage to the barrier is 23 kV.

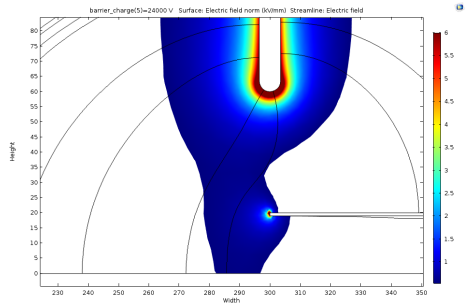

(d) Applied voltage to the barrier is 24 kV.

Figure 4.7: Field distributions with applied breakdown voltage U_{BD} on the rod. The white area signifies the region where the electric field $E_{norm} \geq 0.54$ $\frac{kV}{mm}$. The color code ranges 0.54 (dark blue) to 6 from $\frac{kV}{mm}$ (dark red). Figures (a) to (d) show applied rod voltage $U_{BD} = 75$ kV, barrier height $d = 20$ mm, barrier protrusion $p = 0$ mm, barrier thickness, $t = 1$ mm.

is 2.8 mm. For all the streamer inception voltages the integrated length of the field line was calculated. None of the integration paths in this script ever exceeded 4 mm before the script resulted in streamer inception. The inception voltages in the column with 0 mm protrusions follow the same trend as the withstand voltages in the similar configuration. This similar trend suggests the field enhancement at the edge of the barrier is an important parameter for the withstand as well as breakdown voltages. For the 0 mm protrusion configurations the edge of the barrier is closest to the rod tip compared to similar barrier heights and different protrusions.

Comparing the calculated inception voltages and the observed withstand voltages shows that the withstand voltage is not determined by the streamer inception voltage. The electric field is strongly inhomogeneous for all the configurations, and the

Table 4.4: Calculated barrier charge required to obtain a contiguous electrical field with field strength $E_{norm} \geq 0.54\ \frac{kV}{mm}$. The voltage applied to the rod in the configurations are the breakdown voltages observed experimentally (table 4.1). The calculations are done for varying values of barrier protrusion, p, and barrier height from the ground, d, with constant barrier thickness 1 mm. The sweeps are done in increments of 1 kV.

Barrier height, d	Charge applied to the barrier [kV]		
	p = 0 mm	p = 20 mm	p = 40 mm
20	23	24	52
30	34	37	47
40	47	52	45
50	63	67	70

streamer inception voltage only represents the first stage of the breakdown process.

The lowest streamer inception voltage, indicates the voltage level where discharge activity starts. The initial streamers will travel down towards the barrier and start charging the barrier, as seen in figures 4.6 and 4.7. However, the initial streamers, even if they reach ground are not necessarily sufficient to achieve a breakdown [16]. By allowing the barrier to be charged by a small amount, the calculated streamer inception voltage will increase drastically for the next "generation" of streamers. By continuing this process it might be possible to simulate a series of steps of streamer inceptions, barriers charging, and then new streamer inceptions, eventually finding the breakdown voltage. This, however, requires more educated assumptions on what the actual charge of a barrier is during the different stages of the breakdown process. In figure C.2 and attempt is made to look at the voltage inception with charge applied to the barrier. In this case the barrier was charged with 300 volts applied to the top and sides of the barrier. The initial voltage distribution is directly affecting the field distribution. When the MATLAB script in appendix B.2 starts to scale the field, the contribution from the charge on the barrier is scaled linearly as well. The result is a much higher calculated inception voltage. This shows how a charging of the barrier can help simulate the different stages of the breakdown with "simple" tools such as MATLAB and COMSOL.

4.4 Sources of error

4.4.1 Barrier placements and gap distances

During the tests the barriers were cleaned with isopropyl alcohol between each test. This cleaning process could move the barrier somewhat leading to small variations between the different shots. However, the distance was controlled regularly so this phenomenon should not represent a large source of error.

A slight mechanical sagging was observed in the Lexan barriers. This sagging

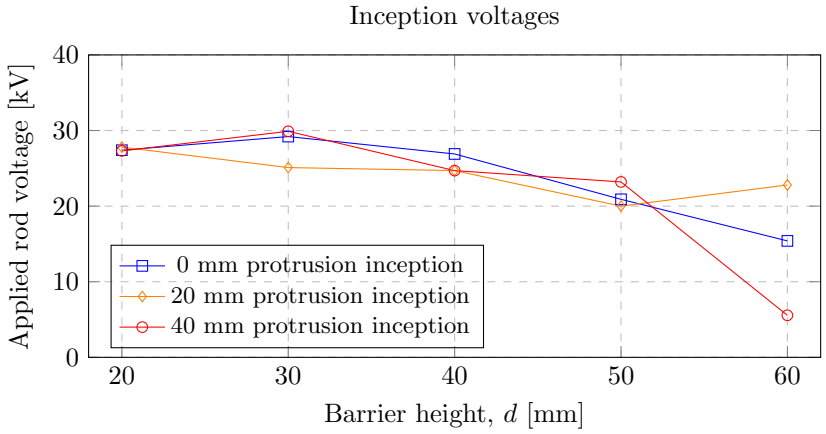

Figure 4.8: Calculated inception voltages for the configurations with 0, 20 and 40 mm barrier protrusions. The barrier thickness is kept at 1 mm. The results can also be seen in table 4.5.

Table 4.5: Calculated rod voltages needed to instigate streamer inception according to [1]. The calculations are done for varying values of barrier protrusion, p, and barrier height from the ground, d. The barrier thickness is kept constant at 1 mm. Background field calcultations are conducted in COMSOL and post processed in MATLAB. The results can also be seen in figure 4.8.

Barrier height, d	Applied rod voltage at first streamer inception [kV]		
	p = 0 mm	p = 20 mm	p = 40 mm
20	27.4	27.8	27.3
30	29.2	25.1	29.9
40	26.9	24.7	24.7
50	20.9	20.0	23.2
60	15.4	22.8	5.56

was more pronounced towards the centre of the barrier furthest from the support pieces at the edges. Such a sag represents a deviation in the gap distance that is consistent throughout the tests conducted in this thesis.

4.4.2 Oscilloscope readings

For the majority of the tests the coarseness of the oscilloscope was set to 5 V per square in order to capture the entire applied impulse. This can be seen in figure 3.2. When using this resolution on the scope the smallest increment the cursors could be moved was 0.2 volts. Using equation 3.3 this translates to $\sim$ 1 kV in pure uncertainty. Having in mind the applied voltage impulses was adjusted in increments of $\Delta V = 2.5$ kV, this uncertainty of 1 kV may represent an error, as

2.5 kV could be read either as 2 kV or 3 kV. This is an error that may not be compensated for in the $n = 20$ shots per test. This uncertainty is a property of the oscilloscope, so adjusting the measuring circuit in section 3.3 would not mitigate the problem. It was not possible to acquire a more precise oscilloscope. Also, using the peak to peak measuring would capture top value of the damping response seen in figure 3.2b.

4.4.3 Component values

The scaling of the actual voltages versus the voltages measured on the scope may be influenced by the values of the components seen in figure 3.3. These components were never measured to confirm the given values. However, since the travelling wave was properly terminated, one can assume the sum of R_3 and R_4 was equal to Z_k.

4.4.4 Surface charge

Each impulse shot caused surface charge accumulation on the barrier surface. The barrier was cleaned of charges between each shot, but the measurement after the cleaning was done by hand and may be subject to human error. It is not inconceivable that some surface charge may have left on the barrier.

4.4.5 Standard deviations and breakdown regions

Certain breakdown voltage tests were rather troublesome to conduct. Some of the measurements had unacceptable standard deviations, more than 4 [kV], for no apparent reason. These test were re-done resulting acceptable standard deviations. During some of the tests it was difficult to find the correct region of breakdown. Some initial findings resulted in a much lower breakdown voltage, only for the breakdown voltage to increase again. One of these tests can be seen in figure F.1. The values in figure F.1 were obtained during a single day with negligible changes in humidity, temperature and air pressure.

Chapter 5

Conclusion

The goal of this thesis is to gain insight in the mechanisms behind a breakdown in a plane-rod gap with an insulating barrier under high voltage impulse conditions. To have an experimental background a set of configurations with varying barrier height and protrusion was tested in the high voltage lab. During these tests, the distance between the rod and the ground electrode was kept constant at 60 mm, in order to quantify the effect of the barrier.

In order to try and explain the observed results, the test rig was built in 3D in COMSOL to analyse electric field distributions. To quantify the amount of charge needed on the barrier to grow the region with propagation field strength $E_{st} = 0.54$ $\frac{kV}{mm}$ down to ground, a parametric sweep was conducted for all barrier configurations. The field distributions were post processed in MATLAB, and the streamer inception voltage was calculated from extracted electric field line data. This was done to examine the field distribution's effect on the formation of streamers, which is the mechanism behind breakdown in impulse conditions.

In general, the withstand voltage increases with increasing barrier protrusion. This is explained, in part, by the increasing shortest geometrical distance, x_s from the high voltage electrode to ground. There is no general optimal barrier height among the different protrusions. The 0 mm protrusion performs best at a 30 mm barrier height, or $\frac{d}{d+d'} = \frac{1}{2}$. The 20 mm barrier protrusion configurations perform best at a barrier height of 40 mm, or $\frac{d}{d+d'} = \frac{2}{3}$. The proposed explanation for this is that the electric field enhancement is strongest at the edge of the barrier, due to charge accumulation. This field enhancement weakens the field strength between the rod and the barrier. This requires the applied rod voltage to be higher to compensate for the weakening caused by the charge accumulated on the barrier. The best performing of the barrier configurations overall is when the barrier protrusion is 40 mm from the centre of the rod, and the barrier height is 50 mm from the ground. This coincides with the longest of the shortest geometrical distance x_s, ignoring the distance when the barrier is touching the rod. The fact that the longest x_s gives the best performance suggests that the The best performing configuration has a

relationship with the gap distance, d+d'= 60 mm, when the protrusion relation is $\frac{p}{d+d'} = \frac{2}{3} = 0.67$, and the height relation is $\frac{d}{d+d'} = \frac{5}{6} = 0.83$. This configuration improves the withstand voltage with 28% compared to a barrier-less gap. The results can be estimated with a 10 % lower predicted withstand voltage for the 40 mm protruding barriers. Here, the length of the path to ground, x_s, seems to be more significant than the distortions in the electric field from the barrier.

The streamer inception voltage is not affected a great deal in the calculations conducted in this thesis. This is because the background field is not influenced a lot by the presence of a barrier. By applying charge to the barrier, a larger influence can be seen in the inception voltage as a function of the barrier configurations. However, a more educated starting point for the simulations in terms of the relation between the rod and the barrier charge is needed.

Chapter 6

Further Work

In this thesis it has been proposed that the streamer inception voltage can be manipulated by applying a voltage potential to the barrier in COMSOL before extracting the field line data to MATLAB. The idea is that as the barrier charges, the background field is affected, which again can affect the streamer inception voltage. When this is done, a step wise simulation can be done in MATLAB, returning the true withstand voltage from the streamer inception criterion. The charge of the rod was 1 kV and the charge on the barrier was set to 300 V in the initial COMOL calculation. This was a rather arbitrary value for the barrier charge, and could warrant further investigation.

The thickness of the barrier used in this thesis was 1 mm. Similar projects have used barriers with 5 mm thickness. The significance of the barrier thickness could be investigated by comparing pictures of the streamer propagation with a high speed camera. The streamer path should also be documented to investigate the streamer path's dependency in the barrier configurations. This could be done with both a single lens camera and a high speed Imacon camera.

The experiments done in this thesis have been limited to an air gap of 60 mm. It could be of interest to investigate similar configurations and trends for larger air gaps and barrier protrusions.

Bibliography

[1] A Pedersen, T Christen, A Blaszczyk, and H Boehme. Streamer inception and propagation models for designing air insulated power devices. *Annual Report - Conference on Electrical Insulation and Dielectric Phenomena, CEIDP*, pages 604–607, 2009.

[2] Erling Ildstad. *Laboratorieoppgave OV2: generering og fordeling av imulsspenninger*. Institutt for elkraftteknikk, NTNU, 2005.

[3] Jan-Henrik Solbakken. *Multiple barrierer i inhomogene luftgap ved lynoverspenninger*. Institutt for elkraftteknikk, NTNU, 2013.

[4] S M Lebedev, O S Gefle, and Y P Pokholkov. The barrier effect in dielectrics: the role of interfaces in the breakdown of inhomogeneous dielectrics. *Dielectrics and Electrical Insulation, IEEE Transactions on*, 12(3):537–555, 2005.

[5] V. Ramaswamy P. Artaxo T. Berntsen R. Betts D.W. Fahey J. Haywood J. Lean D.C. Lowe G. Myhre J. Nganga R. Prinn G. Raga M. Schulz Forster, P. and R. Van Dorland. Changes in Atmospheric Constituents and in Radiative Forcing. *Climate Change 2007: The Physical Science Basis. Contribution of Working Group I to the Fourth Assessment Report of the Intergovernmental Panel on Climate Change*, 30(22):129–234, 2007.

[6] UNFCCC. Kyoto Protocol To the United Nations Framework Kyoto Protocol To the United Nations Framework. *Review of European Community and International Environmental Law*, 7:214–217, 1998.

[7] Erling Ildstad. *Kompendium TET4160 High Voltage Insulation Materials*. Akademika forlag, 2014.

[8] H. Raether. Die entwicklung der elektronenlawine in den funkenkanal. *Zeitschrift für Physik*, 112(7-8):464–489, 1939.

[9] Leonard B. Loeb and Arthur F. Kip. Electrical discharges in air at atmospheric pressure the nature of the positive and negative point-to-plane coronas and the mechanism of spark propagation. *Journal of Applied Physics*, 10(3):142–160, 1939.

[10] J. M. Meek. A theory of spark discharge. *Phys. Rev.*, 57:722–728, Apr 1940.

[11] Frank Mauseth. Lecture slides from the course TET4160 Insulating Materials for High Voltage Applications. Autumn 2014. Trondheim, 29.08.2014.

[12] Komson Petcharaks. Applicability of the streamer breakdown criterion to inhomogeneous gas gaps. *Ph. D. Thesis No. 11192*, Zurich, 1995.

[13] Jonathan S Jørstad. *Effects of Barriers in Air Insulated Rod-Plane Gaps.* Department of Electric Power Engineering, NTNU, 2012.

[14] F. Mauseth, J. S. Jørstad, and A. Pedersen. Streamer inception and propagation for air insulated rod-plane gaps with barriers. *Annual Report - Conference on Electrical Insulation and Dielectric Phenomena, CEIDP*, pages 729–732, 2012.

[15] Hans Kristian Høydalen. *Kompendium TET4130 Overspenninger og overspenningsvern.* Institutt for elkraftteknikk, 2014.

[16] Hans Kristian Meyer. Frank Mauseth. Atle Pedersen. Jonas Ekeberg. Streamer propagation in rod-plane air gaps with a dielectric barrier. *CEIDP2016*, Trondheim, 2016.

Appendix A

Equipment and serial numbers

Table A.1: Equipment names and serial numbers

Name	Description	Serial number
Tektronix MSO2024B Mixed Signal Oscilloscope	Oscilloscope	G04-0372
T Rek model 520	Electrostatic voltmeter	C05-0022
C_b	Discharge capacitor	K03-0021
Control desk	Impulse generator control desk	B03-0037
T Rek model 354 A ESD Monitor	Electrostatic discharge monitor	C05-0021
T Rek model 354 A ESD Probe	Electrostatic discharge probe	C05-0021-04
prologue IW004/36-5136	Wireless weather station	150985716

Appendix B

MATLAB source code

B.1 Integration of α_{eff}

Listing B.1: Function implementing the streamer inception criterion formulated in equation 2.3. The ionization coefficients are found from [12].

```
function [I, streamer_lenght, I_matrix] = integrateAlpha(E_crit, N_crit)
%INTEGRATEALPHA finds the alpha value along a field line according to ...
    the streamer inception criterion. Based on a script by Atle ...
    Pedersen, SINTEF Energy Research.
matrix_size = size(E_crit)-1;
I = 0;
I_matrix = zeros(matrix_size(1,1), 1);
step_matrix = 0;
step = 0;

for i = 1:matrix_size(1,1)
if I < N_crit
    if E_crit(i,5) >= 2.588 && E_crit(i,5) <= 7.943
        step_matrix(i) = steplength_calc(E_crit, i);
        I_matrix(i) = (1.6053*(E_crit(i,5) - 2.165)^2 - ...
            0.2873)*step_matrix(i);
    elseif E_crit(i,5) > 7.943 && E_crit(i,5) <= 14
        step_matrix(i) = steplength_calc(E_crit, i);
        I_matrix(i) = (16.7766*E_crit(i,5)-80.0006)*step_matrix(i);
    elseif E_crit(i,5) > 14
        step_matrix(i) = steplength_calc(E_crit, i);
        I_matrix(i) = (1175*exp(-28.38*E_crit(i,5)))*step_matrix(i);
    end
end

if (I == N_crit) || (I_matrix(i) == 0)
    I_matrix(i) = 0;
    step_matrix(i) = 0;
end

    streamer_lenght = sum(step_matrix);
```

```
29      I = sum(I_matrix);
30  end
31  end
```

B.2 Field scaling function

Listing B.2: The function scaling the electric field strength for each new applied voltage to the rod.

```
1  function E_crit_temp = scaleField(in_matrix, U_old, U_new )
2  %SCALEFIELD scales the electrical field strength of a streamer matrix ...
       to fit a new applied voltage
3  matrix_size = size(in_matrix);
4
5      E_crit_temp = in_matrix;
6
7      for i = 1:matrix_size(1,1)
8          E_crit_temp(i,5) = in_matrix(i,5)*U_new/U_old;
9      end
10 end
```

B.3 Streamer matrix sorting

Listing B.3: The function sorting the extracted field lines and returning the field line with the highest electrical field strength at its beginning.

```
1  function crit_line_data = sort_streamers(x)
2  %Takes in all the streamlines from a file with raw data and returns ...
       the field line with the highest field strength at its starting point.
3  raw_data = x;
4  field_line_number = raw_data(:,4);                %Extracts the column ...
       marked "Streamline"
5  number_of_fieldlines = max(field_line_number)+1; %Finds the number of ...
       field lines in the matrix (starts at 0 and increments by 1)
6
7  data_size = size(raw_data);
8
9  %Loop that finds the first field value in a streamline
10 j=1;
11 i = -1;
12 for n = 2:data_size(1,1)
13     if i ~= raw_data(n,4)                     %Finds the first element ...
           in the streamline column (assumed highest).
14         fieldstrength(j,1) = raw_data(n,5);  %Adds the first "color" ...
               value.
15         fieldstrength(j,2) = n;              %Saves the position of ...
               the first color value in a new streamer coloumn.
16         j = j+1;
17         i = i+1;
18     end
19     n = n+1;
20 end
```

```
21
22 crit_lines = flipud(sortrows(fieldstrength));%Sorting to get the most ...
       critical field strength at the top.
23
24 %Finds the number of rows in the most critical field line.
25 n = crit_lines(1,2);                          %Row index of the fist ...
       element in the most critical field line.
26 i = raw_data(crit_lines(1,2),4);             %The value of the ...
       "streamline" column used to separate streamlines.
27 j = i;
28 while i == j
29     j = raw_data(n,4);
30     n = n+1;
31 end
32
33 crit_line_length = n - crit_lines(1,2)-2; %Number of rows in the most ...
       critical field line.
34 crit_line_data = ...
       raw_data(crit_lines(1,2):crit_lines(1,2)+crit_line_length, 1:5);  ...
       %This matrix now contains the field line with the highest field ...
       strength at its starting point.
35 end
```

B.4 Inception voltage calculation

Listing B.4: The function calculating the streamer inception voltage U. The main function takes in an unprocessed excel-file imported from COMSOL and returns the inception voltage U, the length of the integrated path, the electric field stregth matrix and the streamer constant (in this script called I).

```
1  function [U, streamer_lenght, E_felt, steps_lenght_matrix, I] = ...
       inceptionVoltageCalculate(raw_matrix)
2  E_crit = sort_streamers(raw_matrix);
3
4  U_new = 1000; %[V]
5  U_prev = U_new;
6  U_rod = 1000;
7  N_crit = 18.14; %Critical log(number of electrons) to form a streamer ...
       (ref script from A. Pedersen).
8
9  finished = 0;
10 [I, streamer_lenght, terminate_integral, I_matrix] = ...
       integrateAlpha(E_crit, N_crit);
11
12 while ~finished
13     E_crit_temp = scaleField(E_crit, U_rod, U_new);
14     I = integrateAlpha(E_crit_temp, N_crit);
15
16     if I > N_crit
17         finished = 1;
18         U_new;
19         I;
20
21     elseif U_prev > 300000
```

```
22          disp('Error. No streamer inception at 300 kV. Aborting search.')
23          U = U_prev;
24          return
25
26      else
27          U_prev = U_new;
28          U_new = U_prev+5000;
29          finished = 0;
30      end
31  end
32
33
34   U_upper = U_new;
35   U_lower = U_prev;
36   finish = 0;
37
38   while ~finish
39      U_test = (U_upper + U_lower)/2;
40      E_crit_temp = scaleField(E_crit, U_rod, U_test);
41      [I, streamer_lenght, finish] = integrateAlpha(E_crit_temp, N_crit);
42
43      if I > N_crit
44          U_upper = U_test;
45      else
46          U_lower = U_test;
47      end
48
49      if floor(U_upper) == floor(U_lower)
50          finish = 1;
51      end
52
53      if finish == 1
54          matrix_size = size(E_crit)-1;
55          for i = 1:matrix_size(1,1)
56              E_felt(i) = E_crit_temp(i,5);
57              steps_matrix(i) = steplengthCalc(E_crit, i);
58              steps_lenght_matrix(i) = sum(steps_matrix);
59          end
60      end
61   end
62   U = U_test;
63  end
```

Appendix C

Inception voltage calculations

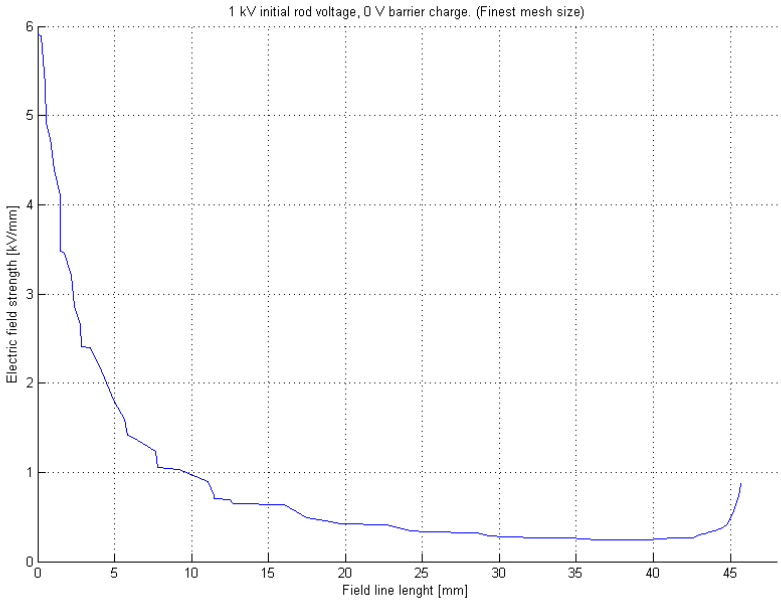

Figure C.1: Plotted electric field strength against the length of the field line. The field distribution is from a configuration with 0 mm barrier protrusion and 30 mm barrier height. The thickness of the barrier is 1 mm. The length of the streamer that contributes to the integral is for this instance 2.8 mm.

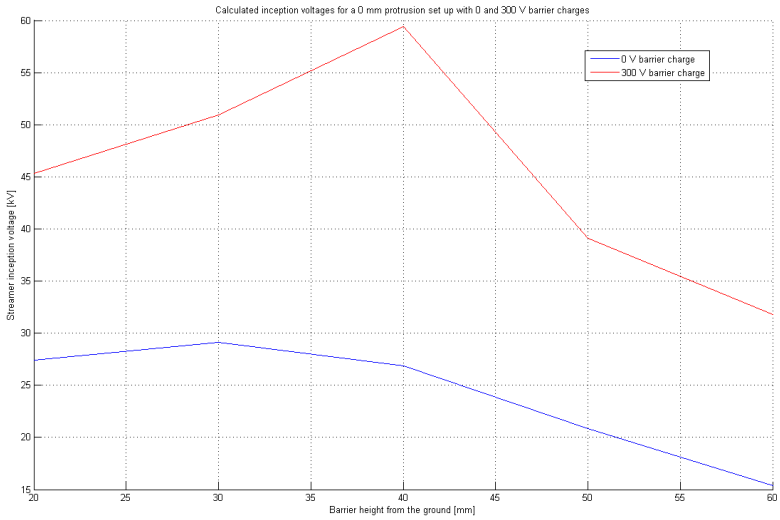

Figure C.2: Inception voltage calculation with basis in a barrier with no charge (blue) and a barrier with a 300 V initial charge (red) in the COMSOL background field calculations. The barrier heights are adjusted from 20 mm to 60 mm in increments of 10 mm. The protrusion is 0 mm and the thickness is 1 mm.

Appendix D

Barrier voltage approximations

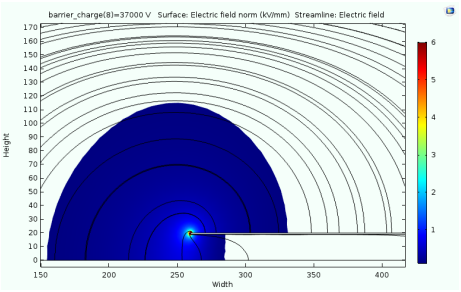

(a) Field distribution (coloured contour plot) and field lines for positive applied voltage. Applied voltage to the barrier is 37 kV.

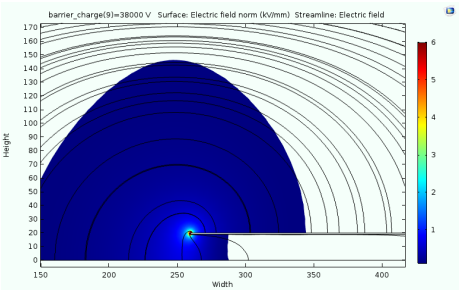

(b) Field distribution (coloured contour plot) and field lines for positive applied voltage. Applied voltage to the barrier is 38 kV.

Figure D.1: The result of a parametric sweep to examine which applied voltage corresponds to the measured field strength after an impulse. The data range shown in blue shows the area where the field strength is 0.115 $\frac{kV}{mm}$, which is the maximum field strength measured after an impulse that did not result in breakdown.

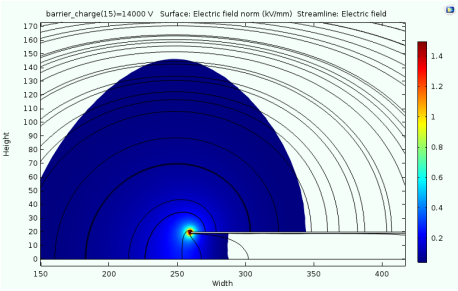

(a) Field distribution (coloured contour plot) and field lines for positive applied voltage. Applied voltage to the barrier is 14 kV.

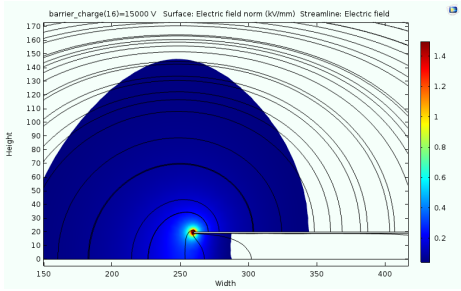

(b) Field distribution (coloured contour plot) and field lines for positive applied voltage. Applied voltage to the barrier is 15 kV.

Figure D.2: The result of a parametric sweep to examine which applied voltage corresponds to the measured field strength after an impulse. The data range shown in blue shows the area where the field strength is 0.043 $\frac{kV}{mm}$, which is the maximum field strength measured after an impulse that did result in breakdown.

Appendix E

Pictures of streamer paths at breakdown

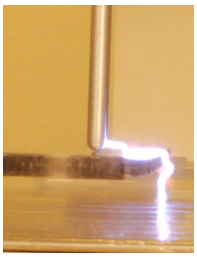

(a) Flash over at gap distance d = 20 mm.

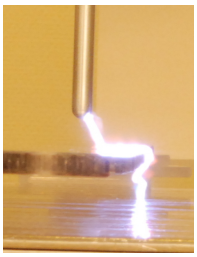

(b) Flash over at gap distance d = 30 mm.

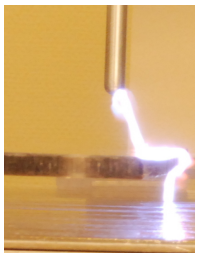

(c) Flash over at gap distance d = 40 mm.

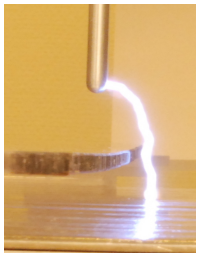

(d) Flash over at gap distance d = 50 mm.

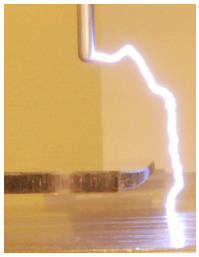

(e) Flash over at gap distance d = 60 mm.

Figure E.1: Photographed streamer paths at flash over for positive voltages. The barrier distance d is fixed to 20 mm. The barrier is protruding 10 mm from the centre of the rod. The thickness of the barrier is 5 mm.

Appendix F

Up- and down-method breakdown regions

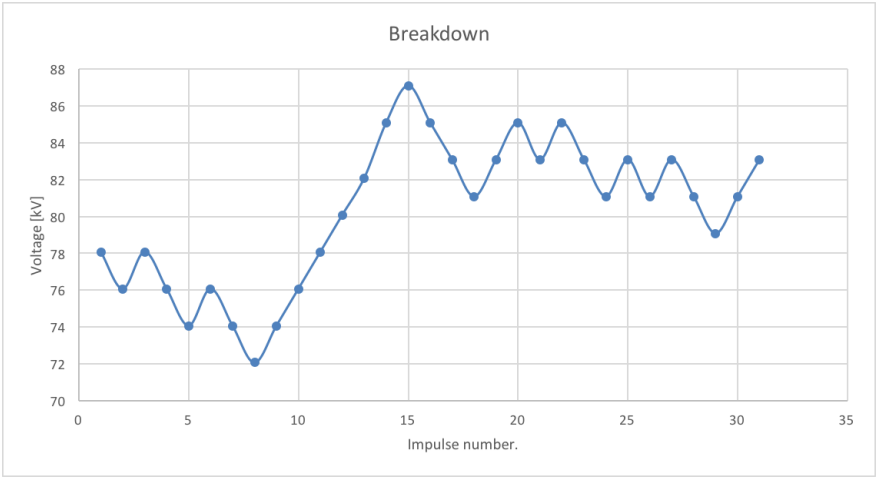

Figure F.1: Example of a test where the region of the breakdown voltage is hard to ascertain. The breakdown voltage seems to drop in the first 7 impulses, then rise by a magnitude of 10 kV.The values were obtained during a single day with negligible changes in humidity and air pressure. The values from this test were rejected.